Physics Letters B 804 (2020) 135377

Contents lists available at ScienceDirect

Physics Letters B

www.elsevier.com/locate/physletb

Measurement of electrons from semileptonic heavy-flavour hadron decays at midrapidity in pp and Pb–Pb collisions at $\sqrt{s_{\rm NN}} = 5.02$ TeV

ALICE Collaboration *

ARTICLE INFO

Article history:
Received 16 November 2019
Received in revised form 8 February 2020
Accepted 17 March 2020
Available online 20 March 2020
Editor: L. Rolandi

ABSTRACT

The differential invariant yield as a function of transverse momentum ($p_{\rm T}$) of electrons from semileptonic heavy-flavour hadron decays was measured at midrapidity in central (0–10%), semi-central (30–50%) and peripheral (60–80%) lead–lead (Pb–Pb) collisions at $\sqrt{s_{\rm NN}} = 5.02$ TeV in the $p_{\rm T}$ intervals 0.5–26 GeV/c (0–10% and 30–50%) and 0.5–10 GeV/c (60–80%). The production cross section in proton–proton (pp) collisions at $\sqrt{s} = 5.02$ TeV was measured as well in $0.5 < p_{\rm T} < 10$ GeV/c and it lies close to the upper band of perturbative QCD calculation uncertainties up to $p_{\rm T} = 5$ GeV/c and close to the mean value for larger $p_{\rm T}$. The modification of the electron yield with respect to what is expected for an incoherent superposition of nucleon–nucleon collisions is evaluated by measuring the nuclear modification factor $R_{\rm AA}$. The measurement of the $R_{\rm AA}$ in different centrality classes allows in-medium energy loss of charm and beauty quarks to be investigated. The $R_{\rm AA}$ shows a suppression with respect to unity at intermediate $p_{\rm T}$, which increases while moving towards more central collisions. Moreover, the measured $R_{\rm AA}$ is sensitive to the modification of the parton distribution functions (PDF) in nuclei, like nuclear shadowing, which causes a suppression of the heavy-quark production at low $p_{\rm T}$ in heavy-ion collisions at LHC.

1. Introduction

The main goal of ALICE is the study of the Quark-Gluon Plasma (QGP), a state of matter which is expected to be created in ultra-relativistic heavy-ion collisions where high temperatures and high energy densities are reached at the LHC [1]. Due to their large masses ($m_{\rm c} \approx 1.5$ GeV/c^2, $m_{\rm b} \approx 4.8$ GeV/c^2), charm and beauty quarks (heavy-flavour) are mostly produced via partonic scattering processes with high momentum transfer, which have typical time scales smaller than the QGP thermalisation time (1 fm/c [2]). Furthermore, additional thermal production, as well as annihilation rates, of charm and beauty quarks in the strongly-interacting matter are expected to be small in Pb–Pb collisions even at LHC energies [3,4]. Consequently, charm and beauty quarks experience the full evolution of the hot and dense medium produced in high-energy heavy-ion collisions, therefore they are ideal probes to investigate the properties of the QGP.

Quarks and gluons interact strongly with the medium and they are expected to lose energy through elastic collisions [5,6] and radiative processes [7,8]. Quarks have a smaller colour coupling factor with respect to gluons, hence the energy loss for quarks is expected to be smaller than that for gluons. In addition, the dead-cone effect is expected to reduce small-angle gluon radiation for heavy quarks with moderate energy to mass ratio [9], thus further attenuating the effect of the medium. The combination of all these effects results in the observed hierarchical mass dependent energy loss [8,10–22].

In order to quantify medium effects on heavy-flavour observables measured in heavy-ion collisions, they are compared with measurements in proton–proton (pp) collisions, where these effects are expected to be absent.

In pp collisions, heavy-quark production can be described by perturbative Quantum Chromodynamics (pQCD) calculations for all transverse momenta, whereas pQCD is not applicable for the calculation of light quark and gluon production at low transverse momenta [3]. Moreover, measurements of heavy-flavour production cross sections in pp collisions provide the necessary experimental reference for heavy-ion collisions.

The medium effects on heavy quarks are quantified through the measurement of the nuclear modification factor, defined as the ratio between the yield of particles produced in ion–ion collisions ($\mathrm{d}^2N_{\rm AA}/\mathrm{d}p_{\rm T}\mathrm{d}y$) and the cross section measured in proton-proton collisions at the same energy ($\mathrm{d}^2\sigma_{\rm pp}/\mathrm{d}p_{\rm T}\mathrm{d}y$), normalised by the average nuclear overlap function $\langle T_{\rm AA}\rangle$:

$$R_{\rm AA}(p_{\rm T}, y) = \frac{1}{\langle T_{\rm AA}\rangle} \cdot \frac{\mathrm{d}^2N_{\rm AA}/\mathrm{d}p_{\rm T}\mathrm{d}y}{\mathrm{d}^2\sigma_{\rm pp}/\mathrm{d}p_{\rm T}\mathrm{d}y}. \quad (1)$$

* *E-mail address:* alice-publications@cern.ch.

https://doi.org/10.1016/j.physletb.2020.135377

The $\langle T_{AA} \rangle$ is defined as the average number of nucleon–nucleon collisions $\langle N_{coll} \rangle$, which can be estimated via Glauber model calculations [23,24], divided by the inelastic nucleon-nucleon cross section. In-medium energy loss shifts the transverse momenta towards lower values, therefore at intermediate and high p_T ($p_T \gtrsim 2$ GeV/c) a suppression of the production is expected ($R_{AA} < 1$). Assuming the total cross section evaluated using $\langle N_{coll} \rangle$ scaling is not modified, the nuclear modification factor is expected to increase towards lower p_T, compensating the depletion at higher momenta. Such a rise was measured by the PHENIX and STAR experiments at RHIC in Au–Au and Cu–Cu collisions at $\sqrt{s_{NN}} = 200$ GeV for electrons from heavy-flavour hadron decays [25–27]. The nuclear modification factor for electrons from semileptonic heavy-flavour hadron decays was also measured by the ALICE collaboration in Pb–Pb collisions at $\sqrt{s_{NN}} = 2.76$ TeV [28,29], where the mentioned trend of R_{AA} was also observed. At low p_T, the nuclear modification factor reaches a maximum around 1 GeV/c and tends to decrease at lower p_T. This trend can be explained by initial and final state effects, like the collective expansion of the hot and dense system [30–32], the interplay between hadronisation via fragmentation and coalescence [22,33,34] and the modification of the parton distribution functions (PDF) inside bound nucleons [35].

Initial-state effects at the LHC are explored with proton–nucleus collisions, where an extended QGP phase is not expected to be formed. The nuclear modification factor of electrons from charm and beauty hadron decays [14,36] and of D mesons [37] in p–Pb collisions at $\sqrt{s_{NN}} = 5.02$ TeV was found to be consistent with unity within uncertainties. From this, one can conclude that the strong suppression observed in Pb–Pb collisions is due to substantial final-state interactions of heavy quarks with the QGP formed in these collisions. However, it is important to note that recently the measurement of the elliptic flow of electrons from semileptonic heavy-flavour hadron decays [38] and of D mesons [39] have been published, showing intriguing and not yet fully understood collective effects in high-multiplicity p–Pb collisions in the heavy-flavour sector.

This paper reports the measurement of the production cross section in pp collisions, the invariant yields and the nuclear modification factor, R_{AA}, in Pb–Pb collisions as a function of p_T of electrons from semileptonic heavy-flavour hadron decays at mid-rapidity at the centre-of-mass energy per nucleon pair $\sqrt{s_{NN}} = 5.02$ TeV. In order to study how the yield and R_{AA} change with centrality in Pb–Pb collisions, the measurement was done in three representative classes: the 0-10% class for central Pb–Pb collisions, the 30-50% for semi-central Pb–Pb collisions and 60-80% for peripheral Pb–Pb collisions.

2. Experimental apparatus and data sample

The ALICE detector is described in detail in Refs. [1,40]. The experiment mainly consists of a central barrel at midrapidity ($|\eta| < 0.9$), embedded in a cylindrical solenoid which provides a magnetic field of 0.5 T parallel to the beam direction, and a muon spectrometer at forward rapidity ($-4 < \eta < -2.5$).

Charged particles produced in the collisions and originating from particle decays are tracked by the Inner Tracking System (ITS) [41] and the Time Projection Chamber (TPC) [42]. The ITS detector, composed of the Silicon Pixel Detector (SPD), Silicon Drift Detector (SDD), and Silicon Strip Detector (SSD), consists of six cylindrical silicon layers surrounding the beam vacuum pipe. These provide measurements of particle momenta and energy loss (dE/dx) used for charged-particle identification (PID), together with the TPC. The particle identification is complemented by a Time-Of-Flight (TOF) [43] detector, which measures the time-of-flight of charged particles. The TOF detector distinguishes electrons from kaons, protons, and pions up to $p_T \simeq 2.5$ GeV/c, $p_T \simeq 4$ GeV/c and $p_T \simeq 1$ GeV/c, respectively. The ElectroMagnetic Calorimeter (EMCal) [44] covers a pseudorapidity region of $|\eta| < 0.7$ and it is used to measure electrons, photons, and jets in an azimuthal region of $\sim 107^o$. The electron identification in the EMCal is based on the measurement of the E/p ratio, where E is the energy of the EMCal cluster matched to the prolongation of the track with momentum p reconstructed with the TPC and ITS detectors. The V0 detectors [45] consist of two arrays of 32 scintillator tiles covering the pseudorapidity ranges $2.8 < \eta < 5.1$ (V0A) and $-3.7 < \eta < -1.7$ (V0C), respectively, and are used for event characterisation.

Table 1
Number of events and $\langle T_{AA} \rangle$ [46,47] used in the analysis, split by collisions system, trigger configuration, and centrality class.

	Centrality	MB	EMCal trigger	$\langle T_{AA} \rangle$ (mb^{-1})
pp	–	881×10^6	–	–
Pb–Pb	0–10%	6×10^6	1.2×10^6	23.26 ± 0.17
	30–50%	12×10^6	0.3×10^6	3.917 ± 0.065
	60–80%	12×10^6	–	0.4188 ± 0.0106

The results presented in this paper are based on data samples of Pb–Pb collisions recorded in 2015 and of pp collisions at the same energy recorded in 2017. The analysed events were collected with a minimum bias (MB) trigger of a logic AND between the V0A and V0C detectors. Pb–Pb collisions were also recorded using the EMCal trigger, which requires an EMCal cluster energy summed over a group of 4×4 calorimeter cells larger than an energy threshold of 10 GeV. The EMCAL triggered events were used for electron measurements for $p_T > 12$ GeV/c. The centrality classes were defined in terms of percentiles of the hadronic Pb–Pb cross section, defined by selections on the sum of the V0 signal amplitudes [46].

For both collision systems, only events with at least two tracks and a reconstructed primary vertex located between ± 10 cm with respect to the nominal interaction point along the z-axis are considered. Events affected by pile-up from different bunch crossings, which constitute less than 1% of the recorded sample, were rejected [28]. The number of events analysed in the two collision systems with the different trigger configurations is summarised in Table 1, together with the average nuclear overlap function $\langle T_{AA} \rangle$ [46,47].

3. Data analysis

The p_T-differential yield of electrons from semileptonic heavy-flavour hadron decays is computed by measuring the inclusive electron yield and subtracting the contribution of electrons that do not originate from semileptonic heavy-flavour hadron decays. In the following, the inclusive electron identification strategy and the subtraction of electrons originating from background sources are described.

3.1. Track selection and electron identification

The selection criteria are similar to the ones described in Refs. [28,29]. They are summarised together with the kinematic cuts applied in the analyses in Table 2.

It is important to note that only tracks that have hits on both SPD layers are accepted so that electrons from late photon conversions in the detector material are significantly reduced. In the Pb–Pb analysis for $p_T > 3$ GeV/c, also tracks with a single hit in the SPD are considered, since the amount of photonic background starts to become negligible. In the analysis in which the EMCal detector is used, specific track-cluster matching criteria are adopted.

As in the procedure followed in Refs. [28,29], electron candidates are identified according to the criteria listed in Table 3. These requirements depend on the data sample and on the transverse momentum interval in which the analyses are performed.

Table 2
Track selection criteria used in the analyses. "DCA" is an abbreviation for "distance of closest approach" of a track to the primary vertex.

Parameter	pp	Pb–Pb ($p_T < 3$ GeV/c)	Pb–Pb ($p_T > 3$ GeV/c)
$\|y\|$	< 0.8	< 0.8	< 0.6
Number of clusters in TPC	≥ 100	≥ 120	≥ 80
TPC clusters in dE/dx calculation	≥ 80	≥ 80	–
Number of clusters in ITS	≥ 3	≥ 4	≥ 3
Minimum number of clusters in SPD	2	2	1
$\|DCA_{xy}\|$	< 1 cm	< 1 cm	< 2.4 cm
$\|DCA_z\|$	< 2 cm	< 2 cm	< 3.2 cm
Found / findable clusters in TPC	> 0.6	> 0.6	> 0.6
χ^2/clusters in TPC	< 4	< 4	< 4
track-cluster matching in EMCal	–	–	$\sqrt{\Delta\varphi^2 + \Delta\eta^2} < 0.02$

Table 3
Electron identification criteria. The following momentum-dependent function is used for the electron identification in pp collisions, based on the TPC dE/dx: $f(p) = \mathrm{Min}(0.12, 0.02 + 0.07p)$. For the electron selection based on clusters in the EMCAL, a criterion on the "σ_s^2" parameter [29], corresponding to the shorter-axis of the shower shape, is used. For brevity, the "low p_T" label is used in place of "$p_T < 3$ GeV/c", as well as "high p_T" in place of "$p_T > 3$ GeV/c".

	Centrality	$n_{\sigma,e}^{TPC}$	$n_{\sigma,e}^{TOF}$	$n_{\sigma,e}^{ITS}$	E/p	Shower shape
pp (low p_T)	–	$[-0.5 + f(p), 3]$	$[-3, 3]$	–	–	–
pp (high p_T)	–	$[0.12, 3]$	–	–	–	–
Pb–Pb (low p_T)	0–10% 30–50% 60–80%	$[-0.16, 3]$ $[0, 3]$ $[0.2, 3]$	$[-3, 3]$	$[-4, 2]$	–	–
Pb–Pb (high p_T)	0–10% 30–50% 60–80%	$[-1, 3]$	–	–	$[0.8, 1.3]$	$0.01 < \sigma_s^2 < 0.35$

The electron identification in pp collisions is performed by evaluating the signal from the TPC and TOF detectors. The discriminant variable in the former detector is the deviation of dE/dx from the parameterised electron Bethe-Bloch [48] expectation value, expressed in units of the dE/dx resolution, $n_{\sigma,e}^{TPC}$, while in the latter one the analogous variable $n_{\sigma,e}^{TOF}$, referring to the particle time-of-flight, is considered. The criterion $|n_{\sigma,e}^{TOF}| < 3$, used for electron identification up to $p_T = 3$ GeV/c, is required to reduce background from kaons and protons. A momentum dependent criterion on $n_{\sigma,e}^{TPC}$ is adopted to guarantee a constant electron identification efficiency of 70% for $p_T < 3$ GeV/c and of 50% for higher transverse momenta by reducing the selection window in $n_{\sigma,e}^{TPC}$, in order to keep the hadron contamination sufficiently low. In the Pb–Pb analysis for $p_T < 3$ GeV/c, the electron identification is performed by applying the same requirement on TOF and due to the large densities of tracks, a selection between $-4 < n_{\sigma,e}^{ITS} < 2$ on the energy deposited in the SDD and SSD detectors is applied in all centrality classes. Finally, the selection on $n_{\sigma,e}^{TPC}$ ensures a constant electron identification efficiency of 50% for all centrality classes. The hadron contamination fraction after the PID is estimated by fitting the $n_{\sigma,e}^{TPC}$ distribution for each particle species with an analytic function in different momentum intervals [28,29]. The inclusive electron sample is then selected by applying a further criterion on $n_{\sigma,e}^{TPC}$, which is chosen in order to have a constant efficiency as a function of the momentum, as well as to have the hadron contamination under control. This criterion is loosened for $p_T > 3$ GeV/c, due to the lower amount of selected hadrons when the EMCal detector is employed.

In the Pb–Pb analysis for $p_T > 3$ GeV/c, the electron candidates are first selected by the measurement of the TPC dE/dx with the criterion $-1 < n_{\sigma,e}^{TPC} < 3$. Then, the selection $0.8 < E/p < 1.3$ on the energy over momentum ratio is applied. Unlike for hadrons, the ratio E/p is close to 1 for electrons because they deposit most of their energy in the EMCal. Furthermore, the electromagnetic showers of electrons are more circular than the ones produced by hadrons. Generally, the shower shape produced in the calorimeter has an elliptical shape which can be characterised by its two axes: σ_l^2 for the long, and σ_s^2 for the short axis. A rather lose selection of $0.01 < \sigma_s^2 < 0.35$ is chosen, since it reduces the hadron contamination while at the same time it does not affect significantly the electron signal [29]. The residual hadron background in the electron sample is evaluated using the E/p distribution for hadron-dominated tracks selected with $n_{\sigma,e}^{TPC} < -3.5$. The E/p distribution of the hadrons is then normalised to match the distribution of the electron candidates in $0.4 < E/p < 0.7$ (away from the true electron peak), so that the fraction of contaminating hadrons under the electron peak can be estimated.

In pp events, the hadron contamination is below 1% at low p_T, while it reaches about 40% at $p_T = 10$ GeV/c. In Pb–Pb, the largest hadron contamination is measured in the most central collisions, where a contamination of about 7% and 10% mainly due to kaon and proton crossing the electron band at $p_T = 0.5$ GeV/c and $p_T = 1$ GeV/c respectively is present. The total hadron contamination contribution amounts to 5% at $p_T = 3$ GeV/c in central events and tends to decrease towards more peripheral collisions. In the EMCal analysis a maximum residual contamination of about 10% is subtracted at the highest transverse momenta in the 0–10% centrality class. In both collision systems, the hadron contamination is subtracted statistically from the inclusive electron candidate yield.

In Pb–Pb collisions, the rapidity ranges used in the ITS-TPC-TOF ($p_T < 3$ GeV/c) and TPC-EMCal ($p_T > 3$ GeV/c) analyses are restricted to $|y| < 0.8$ and $|y| < 0.6$, respectively, to avoid the edges of the detectors, where the systematic uncertainties related to particle identification increase.

3.2. Subtraction of electrons from non heavy-flavour sources

The selected inclusive electron sample does not only contain electrons from open heavy-flavour hadron decays, but also different sources of background:

1. electrons from Dalitz decays of light neutral mesons, mainly π^0 and η, and from photon conversions in the detector ma-

Table 4
Selection criteria for tagging photonic electrons.

Associated electron	pp	Pb–Pb ($p_T < 3$ GeV/c)	Pb–Pb ($p_T > 3$ GeV/c)
p_T^{min} (GeV/c)	0.1	0.1	0.2
$\|y\|$	< 0.8	< 0.8	< 0.9
Number of clusters in TPC	≥ 60	≥ 60	≥ 70
TPC clusters in dE/dx calculation	≥ 60	≥ 60	–
Number of clusters in ITS	≥ 2	≥ 2	≥ 2
$\|DCA_{xy}\|$	< 1 cm	< 1 cm	< 2.4 cm
$\|DCA_z\|$	< 2 cm	< 2 cm	< 3.2 cm
Found / findable clusters in TPC	> 0.6	> 0.6	–
χ^2/d.o.f TPC	< 4	< 4	< 4
$n_{\sigma,e}^{TPC}$	$[-3, 3]$	$[-3, 3]$	$[-3, 3]$
$m_{e^+e^-}$ (MeV/c^2)	< 140	< 140	< 100

terial as well as from thermal and hard scattering processes, called photonic in the following;

2. electrons from weak decays of kaons: $K^{0/\pm} \rightarrow e^{\pm}\pi^{\mp/0}\overset{(-)}{\nu_e}$ (K_{e3});
3. di-electron decays of quarkonia: J/ψ, $\Upsilon \rightarrow e^+e^-$;
4. di-electron decays of light vector mesons: $\omega, \phi, \rho_0 \rightarrow e^+e^-$;
5. electrons from W and Z/γ^*.

The photonic tagging method [21,28,29,36,49] is the technique adopted in the present analyses to estimate the contribution from photonic electrons. With a contribution of 80% to the inclusive electron sample, photonic electrons constitute the main background at $p_T = 0.5$ GeV/c [28]. Their contribution decreases with p_T reaching 25% at about 3 GeV/c. The contribution from di-electron decays of light vector mesons (ρ, ω and ϕ) is negligible compared to the contributions from the photonic sources [50].

Photonic electrons are reconstructed statistically by pairing electron (positron) tracks with opposite charge tracks identified as positrons (electrons), called associated electrons in the following, forming the so-called unlike-sign pairs. The combinatorial background is subtracted using the like-sign invariant mass distribution in the same interval. Associated electrons are selected with the criteria listed in Table 4, which are intentionally looser than the ones applied for the inclusive electron selection, shown in Table 2, in order to maximise the probability to find the photonic partners.

Due to the limited acceptance of the detector and the rejection of some associated electrons by applying the mentioned criteria, a certain fraction of photonic pairs is not reconstructed. Therefore, the raw yield of tagged photonic electrons is corrected for efficiency to find the associated electron (positron), the so called tagging efficiency (ε_{tag}). This is evaluated using Monte Carlo (MC) simulations; pp and Pb–Pb collisions are simulated by the PYTHIA 6 [51] and HIJING [52] event generators, respectively. Primary particle generation is followed by particle transport with GEANT3 [53] and a detailed detector response simulation and reconstruction. The tagging efficiency is defined as the ratio of the number of true reconstructed unlike-sign pair electrons and the number of those generated in the simulations. The simulated p_T distributions of π^0 or η mesons are weighted in MC to match the measured spectra. In both pp and Pb–Pb collisions, the weighting factor for π^0 is provided by using the measured distributions of charged pions [54]. The weighting factor for η mesons is computed using an m_T–scaling approach [55,56]. The total tagging efficiency has a monotonic trend. In pp collisions, it starts at 0.4 for $p_T = 0.5$ GeV/c and rises until $p_T = 3$ GeV/c, where it flattens at 0.7. In Pb–Pb collisions, it follows the same trend, increasing from 0.3 to 0.7 in the same p_T range.

It was observed in the previous analysis [28] that the contribution from J/ψ decays reaches a maximum of around 5% in the region $2 < p_T < 3$ GeV/c in central Pb–Pb collisions, decreasing to a few percent in more peripheral events. At lower and higher momenta, this contribution quickly decreases and becomes negligible, hence it is not subtracted in the present analyses. The associated systematic uncertainty is taken from similar works [28,29]. Due to the requirement of hits in both pixel layers, it was also observed from similar studies in previous measurements [28] that the relative contribution from K_{e3} decays to the electron background is negligible, hence this contribution is not subtracted in the present analyses. Additional sources of background, such as electrons from W and Z/γ^* decays, are subtracted from the fully corrected and normalised electron yield in Pb–Pb collisions at high p_T. These contributions are obtained from calculations using the POWHEG event generator [57] for pp collisions and scaling it by $\langle N_{coll}\rangle$, assuming $R_{AA} = 1$. The contribution from W decays increases from 1% at $p_T = 10$ GeV/c to about 20% at $p_T = 25$ GeV/c in the 0–10% centrality class, while the Z contribution reaches about 10% at the same transverse momentum.

3.3. Efficiency correction and normalisation

After the statistical subtraction of the hadron contamination and the background from photonic electrons, the raw yield of electrons and positrons in bins of p_T is divided by the number of analysed events (N_{ev}^{MB}), by the transverse momentum value at the bin centre p_T^{centre} and the bin width Δp_T, by the width Δy of the covered rapidity interval, by the geometrical acceptance (ε^{geo}) times the reconstruction (ε^{reco}) and PID efficiencies (ε^{eID}), and by a factor of two to obtain the charge averaged invariant differential yield, since in the analyses the distinction between positive and negative charges is not done:

$$\frac{1}{2\pi\, p_T}\frac{d^2N^{e^\pm}}{dp_T dy} = \frac{1}{2}\frac{1}{2\pi\, p_T^{centre}}\frac{1}{N_{ev}^{MB}}\frac{1}{\Delta y \Delta p_T}\frac{N_{raw}^{e^\pm}(p_T)}{(\varepsilon^{geo}\times\varepsilon^{reco}\times\varepsilon^{eID})}. \quad (2)$$

The production cross section in pp collisions is calculated by multiplying the invariant yield of Eq. (2) by the minimum bias trigger cross section at $\sqrt{s} = 5.02$ TeV, that is 50.9 ± 0.9 mb [58]. The per-event yield of electrons from the EMCal triggered sample was scaled to the minimum bias yield by normalisation factors determined with a data-driven method based on the ratio of the energy distributions of EMCal clusters for the two triggers, as described in Ref. [29]. The normalisation is 64.5 ± 0.5 in 0–10% and 246 ± 2.6 in 30–50% centrality intervals, respectively.

The efficiencies are determined using specific MC simulations, where every collision event is produced with at least either a $c\bar{c}$ or $b\bar{b}$ pair and heavy-flavour hadrons are forced to decay semileptonically to electrons [28,29]. The underlying Pb–Pb events were simulated using the HIJING generator [52] and heavy-flavour signals were added using the PYTHIA 6 generator [51]. The efficiency of reconstructing electrons from semileptonic heavy-flavour hadron decays is about 20% at $p_T = 0.5$ GeV/c, then it increases with p_T up to 58% in pp collisions. In Pb–Pb collisions, it follows the same trend, increasing from 5% to 10% in the same p_T range.

3.4. Systematic uncertainties

The overall systematic uncertainties on the p_T spectra are calculated summing in quadrature the different contributions, which are assumed to be uncorrelated. They are summarised in Table 5 and discussed in the following.

The systematic uncertainties on the total reconstruction efficiency arising from the comparison between MC and data are estimated by varying the track selection and PID requirements around the default values chosen in the analyses. The analysis is repeated

Table 5
Contributions to the systematic uncertainties on the cross section (yield) of electrons from heavy-flavour hadron decays in pp (Pb–Pb) collisions, quoted for the transverse momentum intervals $0.5 < p_T < 0.7$ GeV/c and $8 < p_T < 10$ GeV/c. These p_T intervals are listed because the detectors used for particle identification in the two cases are different. In addition, they also represent the first and the last p_T intervals in common for the centrality classes in Pb–Pb collisions, as well as for the pp cross section. At higher p_T the uncertainties are generally lower, apart from the one related to the electroweak background, which stays below 4%. The uncertainties quoted with * are not summed in quadrature together with the others, because they are the R_{AA} normalization uncertainties.

	pp		Pb–Pb (0–10%)		Pb–Pb (30–50%)		Pb–Pb (60–80%)	
p_T (GeV/c)	0.5–0.7	8–10	0.5–0.7	8–10	0.5–0.7	8–10	0.5–0.7	8–10
Track selections	1%	1%	4%	2%	1%	2%	2%	2%
Photonic tagging	4%	–	13%	4%	7%	4%	7%	4%
SPD hit requirement	3%	3%	10%	–	–	–	–	–
J/$\psi\rightarrow$e	–	–	2%	–	2%	–	2%	–
W$\rightarrow$e	–	–	–	<4%	–	<1%	–	<1%
Z/$\gamma^* \rightarrow$e	–	–	–	<1%	–	<1%	–	<1%
$n^{TPC}_{\sigma,e}$ selection	–	5%	–	5%	–	5%	–	2%
E/p selection	–	–	–	6%	–	6%	–	6%
Hadron contamination	–	5%	6%	–	2%	–	–	–
ITS–TPC matching	2%	2%	2%	2%	2%	2%	2%	2%
TPC–TOF matching	2%	–	3%	–	–	–	–	–
η	5%	4%	10%	–	5%	–	5%	–
φ	–	–	10%	–	–	–	–	–
Interaction rate	–	–	5%	–	–	–	–	–
Centrality limit*	–	–	< 1%	< 1%	2%	2%	3%	3%
Luminosity*	2.1%	2.1%	–	–	–	–	–	–
Total uncertainty	9%	9%	24%	9%	9%	9%	9%	8%

with tighter and looser conditions with respect to the default selection criteria and the systematic uncertainty is calculated as the root mean square (RMS) of the distribution of the resulting corrected yields (or cross sections in pp) in each centrality and p_T interval. The systematic uncertainty estimated in pp collisions is less than 2%, while in Pb–Pb collisions it reaches a maximum value of 4% in 0–10% centrality class for $p_T < 0.9$ GeV/c.

Similarly, the systematic uncertainty arising from the photonic-electron subtraction technique is estimated as the RMS of the distribution of yields obtained by varying the selection criteria listed in Table 4. In pp collisions this contribution has a maximum of 4% for $0.5 < p_T < 0.7$ GeV/c and then it gradually decreases with increasing p_T, while in the 0–10% Pb–Pb centrality class it is the dominant source of systematic uncertainty, being 13% in the first p_T interval. This systematic uncertainty mainly arises when the invariant mass criterion on the photonic pairs is varied and it reflects the large contribution of photonic electrons in the low-p_T region.

In order to further test the robustness of the photonic electron tagging, the requirement on the number of clusters for electron candidates in the SPD is relaxed in order to increase the fraction of electrons coming from photon conversions in the detector material. A variation of 3% is observed for the measured pp cross section in the full p_T range, while in central Pb–Pb collisions the observed deviation amounts to 10% for $0.5 < p_T < 0.7$ GeV/c, decreasing with increasing p_T. This systematic uncertainty is less relevant in semi-central collisions, and it is compatible with the variation determined in pp measurements for $1.5 < p_T < 3$ GeV/c.

In addition, the systematic uncertainty related to the subtraction of the background electrons from W and Z/γ^* is estimated by propagating 15% of uncertainty, which covers the possible difference between the measurements and the theoretical calculations [59–61]. The uncertainty from the subtraction on the final result, which is relevant only at high p_T, is less than 4% for electrons from semileptonic heavy-flavour hadron decays in central (0–10%) Pb–Pb collisions for $24 < p_T < 26$ GeV/c, and less than 1% in other centrality classes for the same p_T interval. In the pp analysis, a 5% systematic uncertainty is found while varying the selection criterion in the TPC for $p_T > 8$ GeV/c due to the increasing relative amount of hadrons. An additional systematic uncertainty of 5%, related to the precision of the estimated hadron contamination, is assigned for $p_T > 8$ GeV/c. In Pb–Pb collisions, a 10% systematic uncertainty is assigned for $p_T > 12$ GeV/c due to the variation of electron identification in the TPC, while this contribution is within 5% at lower p_T. Moreover, a 6% uncertainty is assigned due to the E/p selection criterion. Finally, for $p_T < 3$ GeV/c, different functional forms are used for the parametrisation of the pion contribution in the fitting procedure adopted to evaluate the hadron contamination. A systematic uncertainty of about 6% is assigned for $p_T < 3$ GeV/c in the 0–10% centrality class, while this contribution decreases for more peripheral collisions.

In the pp (Pb–Pb) analysis, a systematic uncertainty of about 2% (3%) is assigned due to the incomplete knowledge of the efficiency in matching tracks reconstructed in the ITS and TPC and another 2% (5%) for the track matching between TPC and TOF.

The effects due to the presence of non-uniformity in the correction for the space-charge distortion in the TPC drift volume or irregularities in the detector coverage are then evaluated by repeating the analysis in different geometrical regions. In pp collisions, a maximum systematic uncertainty of 5% is estimated from varying the pseudorapidity range used for the cross section measurement. The same value is assigned in the 30–50% and 60–80% Pb–Pb centrality intervals, while a 10% systematic uncertainty is assigned for $0.5 < p_T < 0.7$ GeV/c in the 0–10% centrality interval, due to the larger sensitivity to the electrons from photon conversions. An additional uncertainty of 10% for $p_T < 1$ GeV/c and of 5% up to $p_T = 3$ GeV/c is estimated from varying the azimuthal region in central Pb–Pb collisions. Furthermore, the analysis of Pb–Pb collisions is repeated using different interaction rate regimes. A 5% deviation is observed at low p_T in central Pb–Pb collisions when selecting only high (> 5 kHz) or low (< 5 kHz) interaction rate events.

The uncertainty from the EMCal trigger normalisation in Pb–Pb collisions at $p_T > 12$ GeV/c is estimated as the RMS of the rejection factor values computed at different transverse momenta [29]. The RMS is 4% and assigned as the systematic uncertainty.

The uncertainties on the R_{AA} normalisation are the quadratic sum of the uncertainties on the average nuclear overlap functions in Table 1, the normalisation uncertainty due to the luminosity and the uncertainty related to the determination of the centrality intervals, which reflects the uncertainty on the fraction of the hadronic cross section used in the Glauber fit to determine the centrality [16,62].

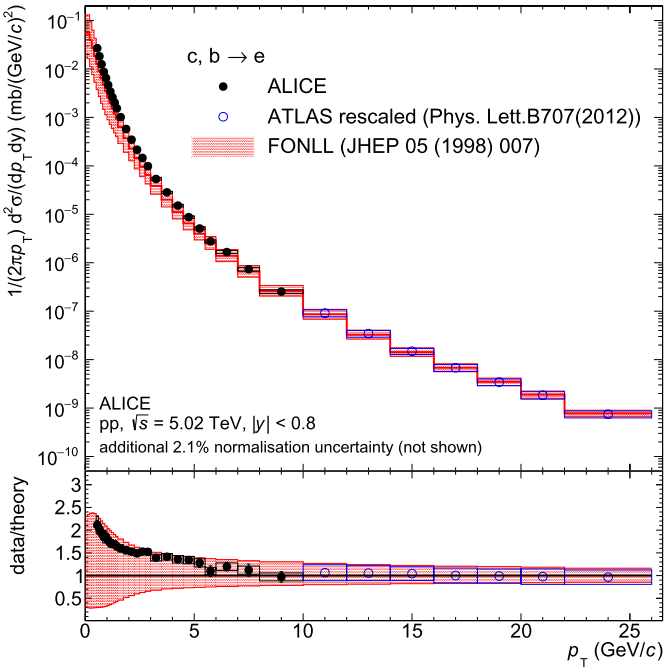

Fig. 1. p_{T}-differential invariant production cross section of electrons from semileptonic heavy-flavour hadron decays in pp collisions at $\sqrt{s} = 5.02$ TeV. The measurement is compared with the FONLL calculation [63]. In the bottom panel, the ratios with respect to the central values of the FONLL calculation are shown. An additional 2.1% normalisation uncertainty, due to the measurement of the minimum bias triggered cross section [46], is not shown in the results.

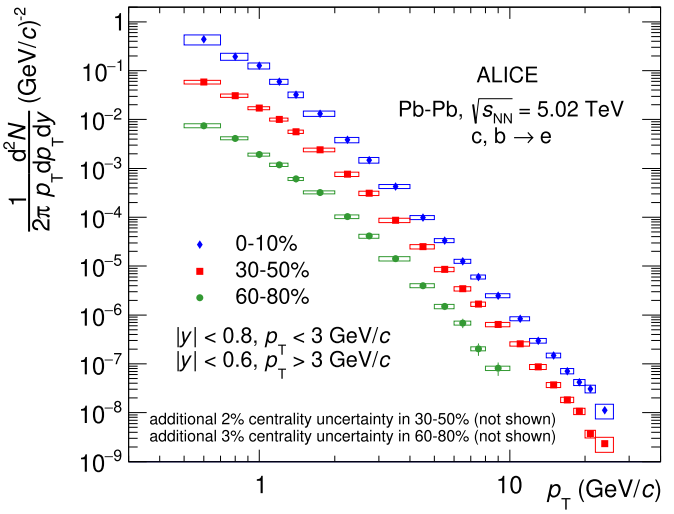

Fig. 2. p_{T}-differential invariant yield in central (0–10%), semi-central (30–50%), and peripheral (60–80%) Pb–Pb collisions at $\sqrt{s_{\mathrm{NN}}} = 5.02$ TeV.

4. Results

4.1. p_{T}-differential cross section in pp collisions and invariant yield in Pb–Pb collisions

The p_{T}-differential production cross section of electrons from semileptonic heavy-flavour hadron decays in pp collisions at $\sqrt{s} = 5.02$ TeV is shown in Fig. 1. The data in the region $0.5 < p_{\mathrm{T}} < 10$ GeV/c is compared with the Fixed-Order-Next-to-Leading-Log (FONLL) [63] pQCD calculation. The uncertainties of the FONLL calculations (dashed area) reflect different choices for the charm and beauty quark masses, the factorisation and renormalisation scales as well as the uncertainty on the set of parton distribution functions (PDF) used in the pQCD calculation (CTEQ6.6 [64]). The measured cross section is close to the upper edge of the theoretical prediction up to $p_{\mathrm{T}} \simeq 5$ GeV/c, as observed in pp collisions at $\sqrt{s} = 2.76$ and 7 TeV [28,49,50], while at higher p_{T}, where electrons from semileptonic beauty hadron decays are expected to dominate, the measurement is close to the mean value of the FONLL prediction.

The p_{T}-differential invariant yield of electrons from semileptonic heavy-flavour hadron decays measured in central (0–10%), semi-central (30–50%), and peripheral (60–80%) Pb–Pb collisions at $\sqrt{s_{\mathrm{NN}}} = 5.02$ TeV is shown in Fig. 2. The measurements are performed in the p_{T} interval 0.5–26 GeV/c in the 0–10% and in the 30–50% centrality intervals, and only up to p_{T} = 10 GeV/c in the 60–80% centrality class due to limited statistics in Pb-Pb data recorded in 2015.

4.2. Nuclear modification factor

The nuclear modification factor of electrons from semileptonic heavy-flavour hadron decays measured in central (0–10%), semi-central (30–50%), and peripheral (60–80%) Pb–Pb collisions at $\sqrt{s_{\mathrm{NN}}} = 5.02$ TeV is shown in Fig. 3. The measured cross section in pp collisions at $\sqrt{s} = 5.02$ TeV (Fig. 1) is used as a reference up to $p_{\mathrm{T}} = 10$ GeV/c. For $p_{\mathrm{T}} > 10$ GeV/c, the reference is obtained by a p_{T}-dependent scaling of the measurement at $\sqrt{s} = 7$ TeV by the ATLAS collaboration [65] with the ratio of the cross section at the two collision energies computed with the FONLL calculation [66]. This ratio is performed by considering the different rapidity coverage of the ATLAS measurement ($|y| < 2$ excluding $1.37 < |y| < 1.52$). The systematic uncertainties of the cross section at $\sqrt{s} = 5.02$ TeV range from 13% to 18% depending on the p_{T} interval, and they are computed as the propagation of the uncertainties associated with FONLL calculations at $\sqrt{s} = 5.02$ TeV and $\sqrt{s} = 7$ TeV and the systematic uncertainties of the ATLAS measurement. The statistical uncertainties are from the ATLAS measurement.

Statistical and systematic uncertainties of the p_{T}-differential yields and cross sections in Pb–Pb and pp collisions, respectively, are propagated as uncorrelated uncertainties. The uncertainties on the R_{AA} normalisation are reported in Fig. 3 as boxes at unity. The measured R_{AA} shows a clear dependence on the collision centrality, since in most central events it reaches a minimum of about 0.3 around $p_{\mathrm{T}} = 7$ GeV/c, while moving to more peripheral Pb–Pb collisions the R_{AA} gets closer to unity at $p_{\mathrm{T}} > 3$ GeV/c. Such a suppression is not observed in proton-lead collisions at the same energy where the QGP is not expected to be formed and the nuclear modification factor is consistent with unity [14,36,37]. Thus the suppression of electron production is due to final-state effects, such as partonic energy loss in the medium. Since electrons from semileptonic beauty decays are expected to dominate the spectrum at high p_{T} while charm production dominates at low p_{T} [14], the measurements show that charm and beauty quarks lose energy in the medium. The centrality dependence of the R_{AA} is compatible with the hypothesis of a partonic energy loss dependence on medium density, being larger in a hotter and denser QGP, like the one created in the most central collisions. In addition, it reflects a path-length dependence of energy loss. Moreover, it has been shown in Refs. [67,68] that a centrality selection bias is present in peripheral Pb–Pb collisions which reduces the R_{AA} below unity even in the absence of any nuclear modification effects. This effect may be responsible for a significant part of the apparent suppression seen in the R_{AA} of electrons from semileptonic heavy-flavour hadron decays in the 60-80% centrality class.

For $p_{\mathrm{T}} < 7$ GeV/c, the R_{AA} of electrons from semileptonic heavy-flavour hadron decays increases with decreasing p_{T} as a consequence of the scaling of the total heavy-flavour yield with

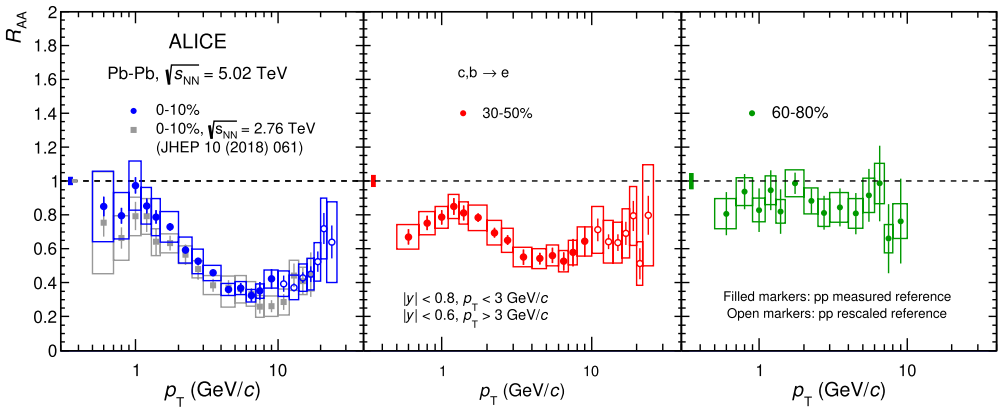

Fig. 3. Nuclear modification factor of electrons from semileptonic heavy-flavour hadron decays measured in the three centrality intervals in Pb–Pb collisions at $\sqrt{s_{NN}} = 5.02$ TeV.

the number of binary collisions among nucleons in Pb–Pb collisions. On the other hand, the nuclear modification factor at low p_T does not rise above unity. This kinematic region is sensitive to the effects of nuclear shadowing: the depletion of parton densities in nuclei at low Bjorken x values can reduce the heavy-quark production cross section per binary collision in Pb–Pb with respect to the pp case [28]. This initial-state effect is studied in p–Pb collisions, however, the present uncertainties on the R_{pPb} measurement do not allow quantitative conclusions on the modification of the PDF in nuclei in the low p_T region to be made [36]. Furthermore, the amount of electrons from semileptonic heavy-flavour hadron decays is reduced due to the presence of hadrochemistry effects. For example, Λ_c^+ baryons decay into electrons with a branching ratio of 5%, while for the D mesons the branching ratio is less than 10%. Since in Pb–Pb collisions more charm quarks might hadronize into baryons [69], this effect reduces the total amount of electrons from semileptonic heavy-flavour hadron decays. Additional effects, such as collective motion induced by the medium, also have an influence on the measured R_{AA}. Also, it has been observed that the radial flow can provoke an additional yield enhancement at intermediate p_T [70–73]. In this case, the radial flow pushes up slow particles to higher momenta, causing a small increase in the nuclear modification factor around $p_T = 1$ GeV/c.

It should be noted that the R_{AA} measurements in the most central collisions at $\sqrt{s_{NN}} = 2.76$ TeV [28] and 5.02 TeV are compatible within uncertainties, as shown in Fig. 3. This effect was predicted by the Djordjevic model [74], and it results from the combination of a higher medium temperature at 5.02 TeV, which would decrease the R_{AA} by about 10%, with a harder p_T distribution of heavy quarks at 5.02 TeV, which would increase the R_{AA} by about 5% if the medium temperature were the same as at 2.76 TeV. An analogous behaviour between the measured R_{AA} at the two energies is also observed for the D mesons [16].

4.3. Comparison with model predictions

In Fig. 4 the measured R_{AA} in the 0–10% (left panel) and 30–50% (right panel) centrality intervals are compared with model calculations [74–81]. The model calculations take into account different hypotheses about mass dependence of energy loss processes, transport dynamics, charm and beauty quark interactions with the QGP constituents, hadronisation mechanisms of heavy quarks in the plasma, and heavy-quark production cross section in nucleus–nucleus collisions.

Most of the models provide a fair description of the data in the region $p_T < 5$ GeV/c in both centrality classes, except for BAMPS [76]. The predictions from the MC@sHQ+EPOS2 [81], PHSD [77], TAMU [78], and POWLANG [80] models also include nuclear modification of the parton distribution functions, which is necessary to predict the observed suppression of the R_{AA} at low p_T. The following observations about the comparison with model calculations are fully in agreement with what is observed in the R_{AA} measurements of D mesons [16].

The nuclear modification factor for central Pb–Pb collisions is well described by the TAMU [78] prediction at $p_T < 3$ GeV/c within the uncertainties related to the shadowing effect on charm quarks. However, this model tends to overestimate the R_{AA} for $p_T > 3$ GeV/c, probably due to the missing implementation of the radiative energy loss in the model, which may become the dominant energy loss mechanism at high p_T.

The agreement with TAMU [78] at low p_T, on the other hand, confirms the dominance of elastic collisions at low momenta, together with the importance of the inclusion of shadowing effects in the model calculations [35], which reduce the total heavy-flavour production in Pb–Pb collisions with respect to an expectation from the binary scaling.

In semi-central Pb–Pb collisions the TAMU [78] and POWLANG [80] predictions are close to the lower edge of the uncertainties of the measured R_{AA} for $p_T < 3$ GeV/c. The latter calculation describes the data better up to $p_T \simeq 8$ GeV/c, while the former provides a good description even at higher transverse momenta. The CUJET3.0 [75] and Djordjevic [74,79] models provide a good description of the R_{AA} within the uncertainties in both centrality intervals for $p_T > 5$ GeV/c, suggesting that the dependence of radiative energy loss on the path length in the hot and dense medium is well understood.

5. Conclusions

The invariant yield of electrons from semileptonic heavy-flavour hadron decays was measured in central (0–10%), semi-central (30–50%), and peripheral (60–80%) Pb–Pb collisions at $\sqrt{s_{NN}} = 5.02$ TeV. The measurement of the nuclear modification factor in all the centrality classes for $p_T < 10$ GeV/c is provided using as reference the cross section measured in pp collisions at the same centre-of-mass energy. The systematic uncertainties of this measurement are reduced by a factor of about 2 compared to the published reference in pp collisions at $\sqrt{s} = 2.76$ TeV [28] and the measured cross section is close to the upper edge of the FONLL uncertainty band. At higher p_T the reference is obtained by a p_T-dependent scaling of the measurement at $\sqrt{s} = 7$ TeV by the ATLAS collaboration [65] with the ratio of the cross section at the two collision energies computed with the FONLL calculation [66]. As in the Pb–Pb analysis at $\sqrt{s_{NN}} = 2.76$ TeV [28,29], the main source of background electrons, constituted by photonic electrons,

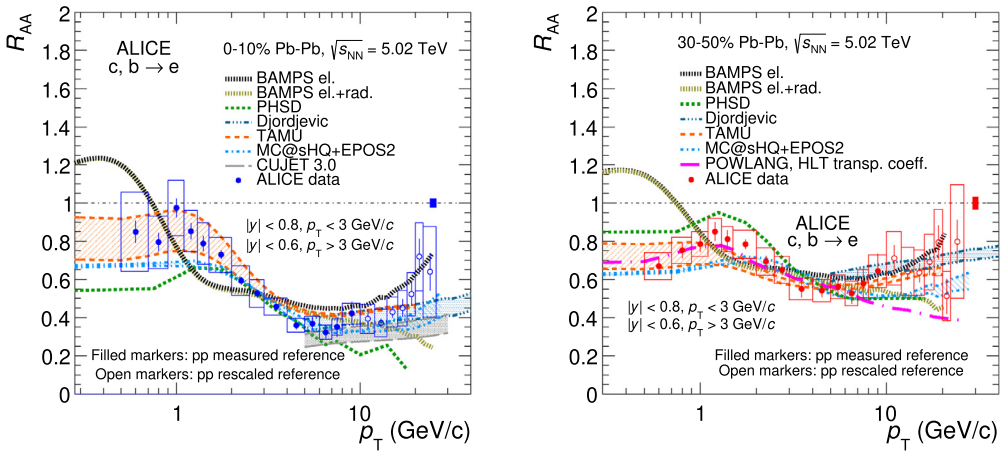

(a) 0–10% (b) 30–50%

Fig. 4. Nuclear modification factor of electrons semileptonic from heavy-flavour hadron decays measured in 0–10% and 30–50% centrality in Pb–Pb collisions at $\sqrt{s_{NN}} = 5.02$ TeV compared with model predictions [74–81].

is removed via the photonic tagging method. In addition, compared with the measurements performed in pp and Pb–Pb collisions at 2.76 TeV, the p_T range is extended, and an additional centrality class is added.

The measured R_{AA} confirms the evidence of a strong suppression with respect to what is expected from a simple binary scaling for large p_T. This is a clear signature of the medium induced energy loss on heavy quarks traversing the QGP produced in heavy-ion collisions.

The measurement of electrons from semileptonic heavy-flavour hadron decays in different centrality classes exhibits the dependence of energy loss on the path length and energy density in the hot and dense medium. The R_{AA} at high p_T (above 5 GeV/c) is fairly described in the 0–10% and 30–50% centrality intervals by model calculations that include both radiative and collisional energy loss. This indicates that the centrality dependence of radiative energy loss is theoretically understood. Further investigations and measurement of electrons from semileptonic decays of beauty hadrons will give more information about the mass dependence of the energy loss in the heavy-flavour sector.

With the good precision of the results presented here, the Pb–Pb data exhibit their sensitivity to the modification of the PDF in nuclei, like nuclear shadowing, which causes a suppression of the heavy-quark production in heavy-ion collisions. The implementation of the nuclear modification of the PDF in theoretical calculations is a necessary ingredient in order for the model predictions to correctly describe the measured R_{AA} [28].

Declaration of competing interest

The authors declare that they have no known competing financial interests or personal relationships that could have appeared to influence the work reported in this paper.

Acknowledgements

The ALICE Collaboration would like to thank all its engineers and technicians for their invaluable contributions to the construction of the experiment and the CERN accelerator teams for the outstanding performance of the LHC complex. The ALICE Collaboration gratefully acknowledges the resources and support provided by all Grid centres and the Worldwide LHC Computing Grid (WLCG) collaboration. The ALICE Collaboration acknowledges the following funding agencies for their support in building and running the ALICE detector: A.I. Alikhanyan National Science Laboratory (Yerevan Physics Institute) Foundation (ANSL), State Committee of Science and World Federation of Scientists (WFS), Armenia; Austrian Academy of Sciences, Austrian Science Fund (FWF): [M 2467-N36] and Österreichische Nationalstiftung für Forschung, Technologie und Entwicklung, Austria; Ministry of Communications and High Technologies, National Nuclear Research Center, Azerbaijan; Conselho Nacional de Desenvolvimento Científico e Tecnológico (CNPq), Financiadora de Estudos e Projetos (Finep), Fundação de Amparo à Pesquisa do Estado de São Paulo (FAPESP) and Universidade Federal do Rio Grande do Sul (UFRGS), Brazil; Ministry of Education of China (MOEC), Ministry of Science & Technology of China (MSTC) and National Natural Science Foundation of China (NSFC), China; Ministry of Science and Education and Croatian Science Foundation, Croatia; Centro de Aplicaciones Tecnológicas y Desarrollo Nuclear (CEADEN), Cubaenergía, Cuba; Ministry of Education, Youth and Sports of the Czech Republic, Czech Republic; The Danish Council for Independent Research | Natural Sciences, the Villum Fonden and Danish National Research Foundation (DNRF), Denmark; Helsinki Institute of Physics (HIP), Finland; Commissariat à l'Énergie Atomique (CEA), Institut National de Physique Nucléaire et de Physique des Particules (IN2P3) and Centre National de la Recherche Scientifique (CNRS) and Région des Pays de la Loire, France; Bundesministerium für Bildung und Forschung (BMBF) and GSI Helmholtzzentrum für Schwerionenforschung GmbH, Germany; General Secretariat for Research and Technology, Ministry of Education, Research and Religions, Greece; National Research Development and Innovation Office, Hungary; Department of Atomic Energy, Government of India (DAE), Department of Science and Technology, Government of India (DST), University Grants Commission, Government of India (UGC) and Council of Scientific and Industrial Research (CSIR), India; Indonesian Institute of Science, Indonesia; Centro Fermi - Museo Storico della Fisica e Centro Studi e Ricerche Enrico Fermi and Istituto Nazionale di Fisica Nucleare (INFN), Italy; Institute for Innovative Science and Technology, Nagasaki Institute of Applied Science (IIST), Japanese Ministry of Education, Culture, Sports, Science and Technology (MEXT) and Japan Society for the Promotion of Science (JSPS) KAKENHI, Japan; Consejo Nacional de Ciencia (CONACYT) y Tecnología, through Fondo de Cooperación Internacional en Ciencia y Tecnología (FONCICYT) and Dirección General de Asuntos del Personal Academico (DGAPA), Mexico; Nederlandse Organisatie voor Wetenschappelijk Onderzoek (NWO), Netherlands; The Research Council of Norway, Norway; Commission on Science and Technology for Sustainable Development in the South (COMSATS), Pakistan; Pontificia Universidad Católica del Perú, Peru; Ministry

of Science and Higher Education and National Science Centre, Poland; Korea Institute of Science and Technology Information and National Research Foundation of Korea (NRF), Republic of Korea; Ministry of Education and Scientific Research, Institute of Atomic Physics and Ministry of Research and Innovation and Institute of Atomic Physics, Romania; Joint Institute for Nuclear Research (JINR), Ministry of Education and Science of the Russian Federation, National Research Centre Kurchatov Institute, Russian Science Foundation and Russian Foundation for Basic Research, Russia; Ministry of Education, Science, Research and Sport of the Slovak Republic, Slovakia; National Research Foundation of South Africa, South Africa; Swedish Research Council (VR) and Knut & Alice Wallenberg Foundation (KAW), Sweden; European Organization for Nuclear Research, Switzerland; Suranaree University of Technology (SUT), National Science and Technology Development Agency (NSDTA) and Office of the Higher Education Commission under NRU project of Thailand, Thailand; Turkish Atomic Energy Agency (TAEK), Turkey; National Academy of Sciences of Ukraine, Ukraine; Science and Technology Facilities Council (STFC), United Kingdom; National Science Foundation of the United States of America (NSF) and United States Department of Energy, Office of Nuclear Physics (DOE NP), United States of America.

References

[1] ALICE Collaboration, B. Abelev, et al., Performance of the ALICE Experiment at the CERN LHC, Int. J. Mod. Phys. A 29 (2014) 1430044, arXiv:1402.4476 [nucl-ex].
[2] F.-M. Liu, S.-X. Liu, Quark-gluon plasma formation time and direct photons from heavy ion collisions, Phys. Rev. C 89 (3) (2014) 034906, arXiv:1212.6587 [nucl-th].
[3] R. Averbeck, Heavy-flavor production in heavy-ion collisions and implications for the properties of hot QCD matter, Prog. Part. Nucl. Phys. 70 (2013) 159–209, arXiv:1505.03828 [nucl-ex].
[4] P. Braun-Munzinger, Quarkonium production in ultra-relativistic nuclear collisions: suppression versus enhancement, J. Phys. G 34 (2007) S471-478, arXiv:nucl-th/0701093 [nucl-th].
[5] M.H. Thoma, M. Gyulassy, Quark damping and energy loss in the high temperature QCD, Nucl. Phys. B 351 (3) (1991) 491–506, http://www.sciencedirect.com/science/article/pii/S0550321305800318.
[6] M.H. Thoma, M. Gyulassy, Quark damping and energy loss in the high temperature QCD, Nucl. Phys. B 351 (1991) 491–506.
[7] M. Gyulassy, M. Plumer, Jet quenching in dense matter, Phys. Lett. B 243 (1990) 432–438.
[8] R. Baier, Y.L. Dokshitzer, A.H. Mueller, S. Peigne, D. Schiff, Radiative energy loss and p_T-broadening of high-energy partons in nuclei, Nucl. Phys. B 484 (1997) 265–282, arXiv:hep-ph/9608322 [hep-ph].
[9] Y.L. Dokshitzer, D.E. Kharzeev, Heavy quark colorimetry of QCD matter, Phys. Lett. B 519 (2001) 199–206, arXiv:hep-ph/0106202 [hep-ph].
[10] N. Armesto, C.A. Salgado, U.A. Wiedemann, Medium induced gluon radiation off massive quarks fills the dead cone, Phys. Rev. D 69 (2004) 114003, arXiv:hep-ph/0312106 [hep-ph].
[11] M. Djordjevic, M. Gyulassy, Heavy quark radiative energy loss in QCD matter, Nucl. Phys. A 733 (2004) 265–298, arXiv:nucl-th/0310076 [nucl-th].
[12] B.-W. Zhang, E. Wang, X.-N. Wang, Heavy quark energy loss in nuclear medium, Phys. Rev. Lett. 93 (2004) 072301, arXiv:nucl-th/0309040 [nucl-th].
[13] H. van Hees, V. Greco, R. Rapp, Heavy-quark probes of the quark-gluon plasma at RHIC, Phys. Rev. C 73 (2006) 034913, arXiv:nucl-th/0508055 [nucl-th].
[14] ALICE Collaboration, J. Adam, et al., Measurement of electrons from beauty-hadron decays in p-Pb collisions at $\sqrt{s_{\rm NN}} = 5.02$ TeV and Pb-Pb collisions at $\sqrt{s_{\rm NN}} = 2.76$ TeV, J. High Energy Phys. 07 (2017) 052, arXiv:1609.03898 [nucl-ex].
[15] ALICE Collaboration, J. Adam, et al., Centrality dependence of high-p_T D meson suppression in Pb-Pb collisions at $\sqrt{s_{\rm NN}} = 2.76$ TeV, J. High Energy Phys. 11 (2015) 205, arXiv:1506.06604 [nucl-ex], J. High Energy Phys. 06 (2017) 032, Addendum.
[16] ALICE Collaboration, S. Acharya, et al., Measurement of D^0, D^+, D^{*+} and D_s^+ production in Pb-Pb collisions at $\sqrt{s_{\rm NN}} = 5.02$ TeV, J. High Energy Phys. 10 (2018) 174, arXiv:1804.09083 [nucl-ex].
[17] CMS Collaboration, A.M. Sirunyan, et al., Measurement of the $B^{\pm}$ meson nuclear modification factor in Pb-Pb Collisions at $\sqrt{s_{NN}} = 5.02$TeV, Phys. Rev. Lett. 119 (15) (2017) 152301, arXiv:1705.04727 [hep-ex].
[18] ALICE Collaboration, J. Adam, et al., Inclusive, prompt and non-prompt J/ψ production at mid-rapidity in Pb-Pb collisions at $\sqrt{s_{NN}}$ = 2.76 TeV, J. High Energy Phys. 07 (2015) 051, arXiv:1504.07151 [nucl-ex].
[19] CMS Collaboration, A.M. Sirunyan, et al., Measurement of prompt and non-prompt charmonium suppression in PbPb collisions at 5.02 TeV, Eur. Phys. J. C 78 (6) (2018) 509, arXiv:1712.08959 [nucl-ex].
[20] CMS Collaboration, A.M. Sirunyan, et al., Studies of beauty suppression via non-prompt D^0 mesons in Pb-Pb Collisions at $Q^2 = 4$ GeV^2, Phys. Rev. Lett. 123 (2) (2019) 022001, arXiv:1810.11102 [hep-ex].
[21] ATLAS Collaboration, M. Aaboud, et al., Measurement of the suppression and azimuthal anisotropy of muons from heavy-flavor decays in Pb+Pb collisions at $\sqrt{s_{\rm NN}} = 2.76$ TeV with the ATLAS detector, Phys. Rev. C 98 (4) (2018) 044905, arXiv:1805.05220 [nucl-ex].
[22] A. Andronic, et al., Heavy-flavour and quarkonium production in the LHC era: from proton–proton to heavy-ion collisions, Eur. Phys. J. C 76 (3) (2016) 107, arXiv:1506.03981 [nucl-ex].
[23] R.J. Glauber, G. Matthiae, High-energy scattering of protons by nuclei, Nucl. Phys. B 21 (1970) 135–157.
[24] M.L. Miller, K. Reygers, S.J. Sanders, P. Steinberg, Glauber modeling in high energy nuclear collisions, Annu. Rev. Nucl. Part. Sci. 57 (2007) 205–243, arXiv:nucl-ex/0701025 [nucl-ex].
[25] STAR Collaboration, B.I. Abelev, et al., Transverse momentum and centrality dependence of high-p_T non-photonic electron suppression in Au+Au collisions at $\sqrt{s_{NN}} = 200$ GeV, Phys. Rev. Lett. 98 (2007) 192301, arXiv:nucl-ex/0607012 [nucl-ex], Phys. Rev. Lett. 106 (2011) 159902, Erratum.
[26] PHENIX Collaboration, A. Adare, et al., Heavy quark production in $p+p$ and energy loss and flow of heavy quarks in Au+Au Collisions at $\sqrt{s_{NN}} = 200$ GeV, Phys. Rev. C 84 (2011) 044905, arXiv:1005.1627 [nucl-ex].
[27] STAR Collaboration, L. Adamczyk, et al., Observation of D^0 meson nuclear modifications in Au+Au collisions at $\sqrt{s_{NN}} = 200$ GeV, Phys. Rev. Lett. 113 (14) (2014) 142301, arXiv:1404.6185 [nucl-ex], Phys. Rev. Lett. 121 (22) (2018) 229901, Erratum.
[28] ALICE Collaboration, S. Acharya, et al., Measurements of low-p$_T$ electrons from semileptonic heavy-flavour hadron decays at mid-rapidity in pp and Pb-Pb collisions at $\sqrt{s_{\rm NN}} = 2.76$ TeV, J. High Energy Phys. 10 (2018) 061, arXiv:1805.04379 [nucl-ex].
[29] ALICE Collaboration, J. Adam, et al., Measurement of the production of high-$p_{\rm T}$ electrons from heavy-flavour hadron decays in Pb-Pb collisions at $\sqrt{s_{\rm NN}} = 2.76$ TeV, Phys. Lett. B 771 (2017) 467–481, arXiv:1609.07104 [nucl-ex].
[30] ALICE Collaboration, J. Adam, et al., Elliptic flow of electrons from heavy-flavour hadron decays at mid-rapidity in Pb-Pb collisions at $\sqrt{s_{\rm NN}} = 2.76$ TeV, J. High Energy Phys. 09 (2016) 028, arXiv:1606.00321 [nucl-ex].
[31] ALICE Collaboration, B. Abelev, et al., D meson elliptic flow in non-central Pb–Pb collisions at energy $\sqrt{s_{\rm NN}} = 2.76$ TeV, Phys. Rev. Lett. 111 (2013) 102301, arXiv:1305.2707 [nucl-ex].
[32] H. van Hees, V. Greco, R. Rapp, Heavy-quark probes of the quark-gluon plasma at RHIC, Phys. Rev. C 73 (2006) 034913, arXiv:nucl-th/0508055 [nucl-th].
[33] V. Greco, C.M. Ko, R. Rapp, Quark coalescence for charmed mesons in ultrarelativistic heavy ion collisions, Phys. Lett. B 595 (2004) 202–208, arXiv:nucl-th/0312100 [nucl-th].
[34] A. Andronic, P. Braun-Munzinger, K. Redlich, J. Stachel, Statistical hadronization of charm in heavy ion collisions at SPS, RHIC and LHC, Phys. Lett. B 571 (2003) 36–44, arXiv:nucl-th/0303036 [nucl-th].
[35] K.J. Eskola, H. Paukkunen, C.A. Salgado, EPS09: a new generation of NLO and LO nuclear parton distribution functions, J. High Energy Phys. 04 (2009) 065, arXiv:0902.4154 [hep-ph].
[36] ALICE Collaboration, J. Adam, et al., Measurement of electrons from heavy-flavour hadron decays in p-Pb collisions at $\sqrt{s_{\rm NN}} = 5.02$ TeV, Phys. Lett. B 754 (2016) 81–93, arXiv:1509.07491 [nucl-ex].
[37] ALICE Collaboration, B. Abelev, et al., Measurement of prompt D-meson production in $p-Pb$ collisions at $\sqrt{s_{\rm NN}} = 5.02$ TeV, Phys. Rev. Lett. 113 (23) (2014) 232301, arXiv:1405.3452 [nucl-ex].
[38] ALICE Collaboration, S. Acharya, et al., Azimuthal anisotropy of heavy-flavor decay electrons in p-Pb Collisions at $\sqrt{s_{\rm NN}} = 5.02$ TeV, Phys. Rev. Lett. 122 (7) (2019) 072301, arXiv:1805.04367 [nucl-ex].
[39] CMS Collaboration, A.M. Sirunyan, et al., Elliptic flow of charm and strange hadrons in high-multiplicity pPb collisions at $\sqrt{s_{\rm NN}} = 8.16$ TeV, Phys. Rev. Lett. 121 (8) (2018) 082301, arXiv:1804.09767 [hep-ex].
[40] ALICE Collaboration, K. Aamodt, et al., The ALICE experiment at the CERN LHC, J. Instrum. 3 (2008) S08002.
[41] ALICE Collaboration, K. Aamodt, et al., Alignment of the ALICE Inner Tracking System with cosmic-ray tracks, J. Instrum. 5 (2010) P03003, arXiv:1001.0502 [physics.ins-det].
[42] ALICE Collaboration, J. Alme, Y. Andres, H. Appelshauser, S. Bablok, N. Bialas, et al., The ALICE TPC, a large 3-dimensional tracking device with fast readout for ultra-high multiplicity events, Nucl. Instrum. Methods A622 (2010) 316–367, arXiv:1001.1950 [physics.ins-det].
[43] ALICE Collaboration, F. Carnesecchi, Performance of the ALICE Time-Of-Flight detector at the LHC, J. Instrum. 14 (06) (2019) C06023, arXiv:1806.03825 [physics.ins-det].

[44] ALICE EMCal Collaboration, U. Abeysekara, et al., ALICE EMCal Physics Performance Report, arXiv:1008.0413 [physics.ins-det].
[45] ALICE Collaboration, E. Abbas, et al., Performance of the ALICE VZERO system, J. Instrum. 8 (2013) P10016, arXiv:1306.3130 [nucl-ex].
[46] ALICE Collaboration, Centrality determination in heavy ion collisions, ALICE-PUBLIC-2018-011, https://cds.cern.ch/record/2636623, 2018.
[47] C. Loizides, J. Kamin, D. d'Enterria, Improved Monte Carlo Glauber predictions at present and future nuclear colliders, Phys. Rev. C 97 (5) (2018) 054910, arXiv:1710.07098, Phys. Rev. C 99 (1) (2019) 019901, Erratum.
[48] H. Bethe, Zur Theorie des Durchgangs schneller Korpuskularstrahlen durch Materie, Ann. Phys. 397 (3) (1930) 325–400.
[49] ALICE Collaboration, B. Abelev, et al., Measurement of electrons from semileptonic heavy-flavor hadron decays in pp collisions at $\sqrt{s} = 2.76$ TeV, Phys. Rev. D 91 (1) (2015) 012001, arXiv:1405.4117 [nucl-ex].
[50] ALICE Collaboration, B. Abelev, et al., Measurement of electrons from semileptonic heavy-flavour hadron decays in pp collisions at $\sqrt{s} = 7$ TeV, Phys. Rev. D 86 (2012) 112007, arXiv:1205.5423 [hep-ex].
[51] T. Sjostrand, S. Mrenna, P.Z. Skands, PYTHIA 6.4 Physics and Manual, J. High Energy Phys. 05 (2006) 026, arXiv:hep-ph/0603175 [hep-ph].
[52] M. Gyulassy, X.-N. Wang, HIJING 1.0: a Monte Carlo program for parton and particle production in high-energy hadronic and nuclear collisions, Comput. Phys. Commun. 83 (1994) 307, arXiv:nucl-th/9502021 [nucl-th].
[53] R. Brun, F. Bruyant, F. Carminati, S. Giani, M. Maire, A. McPherson, G. Patrick, L. Urban, GEANT: Detector Description and Simulation Tool; Oct 1994. CERN Program Library. CERN, Geneva, 1993. https://cds.cern.ch/record/1082634. Long Writeup W5013.
[54] ALICE Collaboration, S. Acharya, et al., Production of charged pions, kaons and (anti-)protons in Pb-Pb and inelastic pp collisions at $\sqrt{s_{\rm NN}} = 5.02$ TeV, arXiv:1910.07678 [nucl-ex].
[55] P.K. Khandai, P. Shukla, V. Singh, Meson spectra and m_T scaling in $p+p$, d+Au, and Au + Au collisions at $\sqrt{s_{NN}} = 200$ GeV, Phys. Rev. C 84 (2011) 054904, arXiv:1110.3929 [hep-ph].
[56] L. Altenkämper, F. Bock, C. Loizides, N. Schmidt, Applicability of transverse mass scaling in hadronic collisions at energies available at the CERN Large Hadron Collider, Phys. Rev. C 96 (6) (2017) 064907, arXiv:1710.01933 [hep-ph].
[57] C. Oleari, The POWHEG-BOX, Nucl. Phys. Proc. Suppl. 205–206 (2010) 36–41, arXiv:1007.3893 [hep-ph].
[58] ALICE Collaboration, ALICE 2017 luminosity determination for pp collisions at $\sqrt{s} = 5$ TeV, ALICE-PUBLIC-2018-014, http://cds.cern.ch/record/2648933, Nov 2018.
[59] ATLAS Collaboration, G. Aad, et al., Measurements of the W production cross sections in association with jets with the ATLAS detector, Eur. Phys. J. C 75 (2) (2015) 82, arXiv:1409.8639 [hep-ex].
[60] ATLAS Collaboration, G. Aad, et al., Measurement of the low-mass Drell-Yan differential cross section at $\sqrt{s} = 7$ TeV using the ATLAS detector, J. High Energy Phys. 06 (2014) 112, arXiv:1404.1212 [hep-ex].
[61] CMS Collaboration, A.M. Sirunyan, et al., Measurement of the differential Drell-Yan cross section in proton-proton collisions at $\sqrt{s} = 13$ TeV, J. High Energy Phys. 12 (2019) 059, arXiv:1812.10529 [hep-ex].
[62] ALICE Collaboration, J. Adam, et al., Transverse momentum dependence of D-meson production in Pb-Pb collisions at $\sqrt{s_{\rm NN}} = 2.76$ TeV, J. High Energy Phys. 03 (2016) 081, arXiv:1509.06888 [nucl-ex].
[63] M. Cacciari, M. Greco, P. Nason, The p_T spectrum in heavy flavor hadroproduction, J. High Energy Phys. 05 (1998) 007, arXiv:hep-ph/9803400 [hep-ph].
[64] P.M. Nadolsky, H.-L. Lai, Q.-H. Cao, J. Huston, J. Pumplin, D. Stump, W.-K. Tung, C.P. Yuan, Implications of CTEQ global analysis for collider observables, Phys. Rev. D 78 (2008) 013004, arXiv:0802.0007 [hep-ph].
[65] ATLAS Collaboration, G. Aad, et al., Measurements of the electron and muon inclusive cross-sections in proton-proton collisions at $\sqrt{s} = 7$ TeV with the ATLAS detector, Phys. Lett. B 707 (2012) 438–458, arXiv:1109.0525 [hep-ex].
[66] R. Averbeck, N. Bastid, Z.C. del Valle, P. Crochet, A. Dainese, X. Zhang, Reference heavy flavour cross sections in pp collisions at $\sqrt{s} = 2.76$ TeV, using a pQCD-driven $\sqrt{s}$-scaling of ALICE measurements at $\sqrt{s} = 7$ TeV, arXiv:1107.3243 [hep-ph].
[67] ALICE Collaboration, S. Acharya, et al., Analysis of the apparent nuclear modification in peripheral Pb–Pb collisions at 5.02 TeV, Phys. Lett. B 793 (2019) 420–432, arXiv:1805.05212 [nucl-ex].
[68] C. Loizides, A. Morsch, Absence of jet quenching in peripheral nucleus–nucleus collisions, Phys. Lett. B 773 (2017) 408–411, arXiv:1705.08856 [nucl-ex].
[69] ALICE Collaboration, S. Acharya, et al., Λ_c^+ production in Pb-Pb collisions at $\sqrt{s_{\rm NN}} = 5.02$ TeV, Phys. Lett. B 793 (2019) 212–223, arXiv:1809.10922 [nucl-ex].
[70] M. He, R.J. Fries, R. Rapp, Heavy-quark diffusion and hadronization in quark-gluon plasma, Phys. Rev. C 86 (2012) 014903, arXiv:1106.6006 [nucl-th].
[71] M. He, R.J. Fries, R. Rapp, $\mathbf{D_s}$-meson as quantitative probe of diffusion and hadronization in nuclear collisions, Phys. Rev. Lett. 110 (11) (2013) 112301, arXiv:1204.4442 [nucl-th].
[72] P.B. Gossiaux, J. Aichelin, T. Gousset, V. Guiho, Competition of heavy quark radiative and collisional energy loss in deconfined matter, J. Phys. G 37 (2010) 094019, arXiv:1001.4166 [hep-ph].
[73] P.B. Gossiaux, M. Nahrgang, M. Bluhm, T. Gousset, J. Aichelin, Heavy quark quenching from RHIC to LHC and the consequences of gluon damping, Nucl. Phys. A 904–905 (2013) 992c–995c, arXiv:1211.2281 [hep-ph].
[74] M. Djordjevic, M. Djordjevic, Predictions of heavy-flavor suppression at 5.1 TeV Pb+Pb collisions at the CERN large hadron collider, Phys. Rev. C 92 (2) (2015) 024918, arXiv:1505.04316 [nucl-th].
[75] J. Xu, J. Liao, M. Gyulassy, Bridging soft-hard transport properties of quark-gluon plasmas with CUJET3.0, J. High Energy Phys. 02 (2016) 169, arXiv:1508.00552 [hep-ph].
[76] J. Uphoff, O. Fochler, Z. Xu, C. Greiner, Elastic and radiative heavy quark interactions in ultra-relativistic heavy-ion collisions, J. Phys. G 42 (11) (2015) 115106, arXiv:1408.2964 [hep-ph].
[77] T. Song, H. Berrehrah, D. Cabrera, W. Cassing, E. Bratkovskaya, Charm production in Pb + Pb collisions at energies available at the CERN large hadron collider, Phys. Rev. C 93 (3) (2016) 034906, arXiv:1512.00891 [nucl-th].
[78] M. He, R.J. Fries, R. Rapp, Heavy flavor at the large hadron collider in a strong coupling approach, Phys. Lett. B 735 (2014) 445–450, arXiv:1401.3817 [nucl-th].
[79] M. Djordjevic, M. Djordjevic, LHC jet suppression of light and heavy flavor observables, Phys. Lett. B 734 (2014) 286–289, arXiv:1307.4098 [hep-ph].
[80] A. Beraudo, A. De Pace, M. Monteno, M. Nardi, F. Prino, Heavy flavors in heavy-ion collisions: quenching, flow and correlations, Eur. Phys. J. C 75 (3) (2015) 121, arXiv:1410.6082 [hep-ph].
[81] M. Nahrgang, J. Aichelin, P.B. Gossiaux, K. Werner, Influence of hadronic bound states above T_c on heavy-quark observables in Pb–Pb collisions at the CERN Large Hadron Collider, Phys. Rev. C 89 (1) (2014) 014905, arXiv:1305.6544 [hep-ph].

ALICE Collaboration

S. Acharya [141], D. Adamová [93], S.P. Adhya [141], A. Adler [73], J. Adolfsson [79], M.M. Aggarwal [98], G. Aglieri Rinella [34], M. Agnello [31], N. Agrawal [10,48,53], Z. Ahammed [141], S. Ahmad [17], S.U. Ahn [75], A. Akindinov [90], M. Al-Turany [105], S.N. Alam [141], D.S.D. Albuquerque [122], D. Aleksandrov [86], B. Alessandro [58], H.M. Alfanda [6], R. Alfaro Molina [71], B. Ali [17], Y. Ali [15], A. Alici [10,27,53], A. Alkin [2], J. Alme [22], T. Alt [68], L. Altenkamper [22], I. Altsybeev [112], M.N. Anaam [6], C. Andrei [47], D. Andreou [34], H.A. Andrews [109], A. Andronic [144], M. Angeletti [34], V. Anguelov [102], C. Anson [16], T. Antičić [106], F. Antinori [56], P. Antonioli [53], R. Anwar [125], N. Apadula [78], L. Aphecetche [114], H. Appelshäuser [68], S. Arcelli [27], R. Arnaldi [58], M. Arratia [78], I.C. Arsene [21], M. Arslandok [102], A. Augustinus [34], R. Averbeck [105], S. Aziz [61], M.D. Azmi [17], A. Badalà [55], Y.W. Baek [40], S. Bagnasco [58], X. Bai [105], R. Bailhache [68], R. Bala [99], A. Baldisseri [137], M. Ball [42], S. Balouza [103], R.C. Baral [84], R. Barbera [28], L. Barioglio [26], G.G. Barnaföldi [145], L.S. Barnby [92], V. Barret [134], P. Bartalini [6], K. Barth [34], E. Bartsch [68], F. Baruffaldi [29], N. Bastid [134], S. Basu [143], G. Batigne [114], B. Batyunya [74], P.C. Batzing [21], D. Bauri [48], J.L. Bazo Alba [110], I.G. Bearden [87], C. Bedda [63], N.K. Behera [60], I. Belikov [136], F. Bellini [34], R. Bellwied [125], V. Belyaev [91], G. Bencedi [145], S. Beole [26], A. Bercuci [47], Y. Berdnikov [96], D. Berenyi [145], R.A. Bertens [130], D. Berzano [58], M.G. Besoiu [67],

L. Betev [34], A. Bhasin [99], I.R. Bhat [99], M.A. Bhat [3], H. Bhatt [48], B. Bhattacharjee [41], A. Bianchi [26], L. Bianchi [26,125], N. Bianchi [51], J. Bielčík [37], J. Bielčíková [93], A. Bilandzic [103,117], G. Biro [145], R. Biswas [3], S. Biswas [3], J.T. Blair [119], D. Blau [86], C. Blume [68], G. Boca [139], F. Bock [34,94], A. Bogdanov [91], L. Boldizsár [145], A. Bolozdynya [91], M. Bombara [38], G. Bonomi [140], H. Borel [137], A. Borissov [91,144], M. Borri [127], H. Bossi [146], E. Botta [26], L. Bratrud [68], P. Braun-Munzinger [105], M. Bregant [121], T.A. Broker [68], M. Broz [37], E.J. Brucken [43], E. Bruna [58], G.E. Bruno [33,104], M.D. Buckland [127], D. Budnikov [107], H. Buesching [68], S. Bufalino [31], O. Bugnon [114], P. Buhler [113], P. Buncic [34], Z. Buthelezi [72], J.B. Butt [15], J.T. Buxton [95], S.A. Bysiak [118], D. Caffarri [88], A. Caliva [105], E. Calvo Villar [110], R.S. Camacho [44], P. Camerini [25], A.A. Capon [113], F. Carnesecchi [10], J. Castillo Castellanos [137], A.J. Castro [130], E.A.R. Casula [54], F. Catalano [31], C. Ceballos Sanchez [52], P. Chakraborty [48], S. Chandra [141], B. Chang [126], W. Chang [6], S. Chapeland [34], M. Chartier [127], S. Chattopadhyay [141], S. Chattopadhyay [108], A. Chauvin [24], C. Cheshkov [135], B. Cheynis [135], V. Chibante Barroso [34], D.D. Chinellato [122], S. Cho [60], P. Chochula [34], T. Chowdhury [134], P. Christakoglou [88], C.H. Christensen [87], P. Christiansen [79], T. Chujo [133], C. Cicalo [54], L. Cifarelli [10,27], F. Cindolo [53], M.R. Ciupek [105], J. Cleymans [124], F. Colamaria [52], D. Colella [52], A. Collu [78], M. Colocci [27], M. Concas [58,ii], G. Conesa Balbastre [77], Z. Conesa del Valle [61], G. Contin [59,127], J.G. Contreras [37], T.M. Cormier [94], Y. Corrales Morales [26,58], P. Cortese [32], M.R. Cosentino [123], F. Costa [34], S. Costanza [139], J. Crkovská [61], P. Crochet [134], E. Cuautle [69], L. Cunqueiro [94], D. Dabrowski [142], T. Dahms [103,117], A. Dainese [56], F.P.A. Damas [114,137], S. Dani [65], M.C. Danisch [102], A. Danu [67], D. Das [108], I. Das [108], P. Das [3], S. Das [3], A. Dash [84], S. Dash [48], A. Dashi [103], S. De [49,84], A. De Caro [30], G. de Cataldo [52], C. de Conti [121], J. de Cuveland [39], A. De Falco [24], D. De Gruttola [10], N. De Marco [58], S. De Pasquale [30], R.D. De Souza [122], S. Deb [49], H.F. Degenhardt [121], K.R. Deja [142], A. Deloff [83], S. Delsanto [26,131], P. Dhankher [48], D. Di Bari [33], A. Di Mauro [34], R.A. Diaz [8], T. Dietel [124], P. Dillenseger [68], Y. Ding [6], R. Divià [34], Ø. Djuvsland [22], U. Dmitrieva [62], A. Dobrin [34,67], B. Dönigus [68], O. Dordic [21], A.K. Dubey [141], A. Dubla [105], S. Dudi [98], M. Dukhishyam [84], P. Dupieux [134], R.J. Ehlers [146], D. Elia [52], H. Engel [73], E. Epple [146], B. Erazmus [114], F. Erhardt [97], A. Erokhin [112], M.R. Ersdal [22], B. Espagnon [61], G. Eulisse [34], J. Eum [18], D. Evans [109], S. Evdokimov [89], L. Fabbietti [103,117], M. Faggin [29], J. Faivre [77], A. Fantoni [51], M. Fasel [94], P. Fecchio [31], A. Feliciello [58], G. Feofilov [112], A. Fernández Téllez [44], A. Ferrero [137], A. Ferretti [26], A. Festanti [34], V.J.G. Feuillard [102], J. Figiel [118], S. Filchagin [107], D. Finogeev [62], F.M. Fionda [22], G. Fiorenza [52], F. Flor [125], S. Foertsch [72], P. Foka [105], S. Fokin [86], E. Fragiacomo [59], U. Frankenfeld [105], G.G. Fronze [26], U. Fuchs [34], C. Furget [77], A. Furs [62], M. Fusco Girard [30], J.J. Gaardhøje [87], M. Gagliardi [26], A.M. Gago [110], A. Gal [136], C.D. Galvan [120], P. Ganoti [82], C. Garabatos [105], E. Garcia-Solis [11], K. Garg [28], C. Gargiulo [34], A. Garibli [85], K. Garner [144], P. Gasik [103,117], E.F. Gauger [119], M.B. Gay Ducati [70], M. Germain [114], J. Ghosh [108], P. Ghosh [141], S.K. Ghosh [3], P. Gianotti [51], P. Giubellino [58,105], P. Giubilato [29], P. Glässel [102], D.M. Goméz Coral [71], A. Gomez Ramirez [73], V. Gonzalez [105], P. González-Zamora [44], S. Gorbunov [39], L. Görlich [118], S. Gotovac [35], V. Grabski [71], L.K. Graczykowski [142], K.L. Graham [109], L. Greiner [78], A. Grelli [63], C. Grigoras [34], V. Grigoriev [91], A. Grigoryan [1], S. Grigoryan [74], O.S. Groettvik [22], J.M. Gronefeld [105], F. Grosa [31], J.F. Grosse-Oetringhaus [34], R. Grosso [105], R. Guernane [77], B. Guerzoni [27], M. Guittiere [114], K. Gulbrandsen [87], T. Gunji [132], A. Gupta [99], R. Gupta [99], I.B. Guzman [44], R. Haake [34,146], M.K. Habib [105], C. Hadjidakis [61], H. Hamagaki [80], G. Hamar [145], M. Hamid [6], R. Hannigan [119], M.R. Haque [63], A. Harlenderova [105], J.W. Harris [146], A. Harton [11], J.A. Hasenbichler [34], H. Hassan [77], D. Hatzifotiadou [10,53], P. Hauer [42], S. Hayashi [132], A.D.L.B. Hechavarria [144], S.T. Heckel [68], E. Hellbär [68], H. Helstrup [36], A. Herghelegiu [47], E.G. Hernandez [44], G. Herrera Corral [9], F. Herrmann [144], K.F. Hetland [36], T.E. Hilden [43], H. Hillemanns [34], C. Hills [127], B. Hippolyte [136], B. Hohlweger [103], D. Horak [37], S. Hornung [105], R. Hosokawa [133], P. Hristov [34], C. Huang [61], C. Hughes [130], P. Huhn [68], T.J. Humanic [95], H. Hushnud [108], L.A. Husova [144], N. Hussain [41], S.A. Hussain [15], T. Hussain [17], D. Hutter [39], D.S. Hwang [19], J.P. Iddon [34,127], R. Ilkaev [107], M. Inaba [133], M. Ippolitov [86], M.S. Islam [108], M. Ivanov [105], V. Ivanov [96], V. Izucheev [89], B. Jacak [78], N. Jacazio [27], P.M. Jacobs [78], M.B. Jadhav [48], S. Jadlovska [116], J. Jadlovsky [116], S. Jaelani [63], C. Jahnke [121], M.J. Jakubowska [142], M.A. Janik [142], M. Jercic [97], O. Jevons [109], R.T. Jimenez Bustamante [105], M. Jin [125], F. Jonas [94,144], P.G. Jones [109], J. Jung [68], M. Jung [68], A. Jusko [109], P. Kalinak [64], A. Kalweit [34], J.H. Kang [147], V. Kaplin [91], S. Kar [6], A. Karasu Uysal [76], O. Karavichev [62], T. Karavicheva [62], P. Karczmarczyk [34], E. Karpechev [62], U. Kebschull [73], R. Keidel [46], M. Keil [34], B. Ketzer [42], Z. Khabanova [88], A.M. Khan [6], S. Khan [17], S.A. Khan [141], A. Khanzadeev [96], Y. Kharlov [89], A. Khatun [17], A. Khuntia [49,118], B. Kileng [36], B. Kim [60], B. Kim [133], D. Kim [147], D.J. Kim [126], E.J. Kim [13], H. Kim [147], J. Kim [147], J.S. Kim [40],

J. Kim [102], J. Kim [147], J. Kim [13], M. Kim [102], S. Kim [19], T. Kim [147], T. Kim [147], S. Kirsch [39], I. Kisel [39], S. Kiselev [90], A. Kisiel [142], J.L. Klay [5], C. Klein [68], J. Klein [58], S. Klein [78], C. Klein-Bösing [144], S. Klewin [102], A. Kluge [34], M.L. Knichel [34], A.G. Knospe [125], C. Kobdaj [115], M.K. Köhler [102], T. Kollegger [105], A. Kondratyev [74], N. Kondratyeva [91], E. Kondratyuk [89], P.J. Konopka [34], L. Koska [116], O. Kovalenko [83], V. Kovalenko [112], M. Kowalski [118], I. Králik [64], A. Kravčáková [38], L. Kreis [105], M. Krivda [64,109], F. Krizek [93], K. Krizkova Gajdosova [37], M. Krüger [68], E. Kryshen [96], M. Krzewicki [39], A.M. Kubera [95], V. Kučera [60], C. Kuhn [136], P.G. Kuijer [88], L. Kumar [98], S. Kumar [48], S. Kundu [84], P. Kurashvili [83], A. Kurepin [62], A.B. Kurepin [62], A. Kuryakin [107], S. Kushpil [93], J. Kvapil [109], M.J. Kweon [60], J.Y. Kwon [60], Y. Kwon [147], S.L. La Pointe [39], P. La Rocca [28], Y.S. Lai [78], R. Langoy [129], K. Lapidus [34,146], A. Lardeux [21], P. Larionov [51], E. Laudi [34], R. Lavicka [37], T. Lazareva [112], R. Lea [25], L. Leardini [102], S. Lee [147], F. Lehas [88], S. Lehner [113], J. Lehrbach [39], R.C. Lemmon [92], I. León Monzón [120], E.D. Lesser [20], M. Lettrich [34], P. Lévai [145], X. Li [12], X.L. Li [6], J. Lien [129], R. Lietava [109], B. Lim [18], S. Lindal [21], V. Lindenstruth [39], S.W. Lindsay [127], C. Lippmann [105], M.A. Lisa [95], V. Litichevskyi [43], A. Liu [78], S. Liu [95], W.J. Llope [143], I.M. Lofnes [22], V. Loginov [91], C. Loizides [94], P. Loncar [35], X. Lopez [134], E. López Torres [8], P. Luettig [68], J.R. Luhder [144], M. Lunardon [29], G. Luparello [59], M. Lupi [73], A. Maevskaya [62], M. Mager [34], S.M. Mahmood [21], T. Mahmoud [42], A. Maire [136], R.D. Majka [146], M. Malaev [96], Q.W. Malik [21], L. Malinina [74,iii], D. Mal'Kevich [90], P. Malzacher [105], A. Mamonov [107], G. Mandaglio [55], V. Manko [86], F. Manso [134], V. Manzari [52], Y. Mao [6], M. Marchisone [135], J. Mareš [66], G.V. Margagliotti [25], A. Margotti [53], J. Margutti [63], A. Marín [105], C. Markert [119], M. Marquard [68], N.A. Martin [102], P. Martinengo [34], J.L. Martinez [125], M.I. Martínez [44], G. Martínez García [114], M. Martinez Pedreira [34], S. Masciocchi [105], M. Masera [26], A. Masoni [54], L. Massacrier [61], E. Masson [114], A. Mastroserio [138], A.M. Mathis [103,117], O. Matonoha [79], P.F.T. Matuoka [121], A. Matyja [118], C. Mayer [118], M. Mazzilli [33], M.A. Mazzoni [57], A.F. Mechler [68], F. Meddi [23], Y. Melikyan [91], A. Menchaca-Rocha [71], E. Meninno [30], M. Meres [14], S. Mhlanga [124], Y. Miake [133], L. Micheletti [26], M.M. Mieskolainen [43], D.L. Mihaylov [103], K. Mikhaylov [74,90], A. Mischke [63,i], A.N. Mishra [69], D. Miśkowiec [105], C.M. Mitu [67], A. Modak [3], N. Mohammadi [34], A.P. Mohanty [63], B. Mohanty [84], M. Mohisin Khan [17,iv], M. Mondal [141], M.M. Mondal [65], C. Mordasini [103], D.A. Moreira De Godoy [144], L.A.P. Moreno [44], S. Moretto [29], A. Morreale [114], A. Morsch [34], T. Mrnjavac [34], V. Muccifora [51], E. Mudnic [35], D. Mühlheim [144], S. Muhuri [141], J.D. Mulligan [78,146], M.G. Munhoz [121], K. Münning [42], R.H. Munzer [68], H. Murakami [132], S. Murray [72], L. Musa [34], J. Musinsky [64], C.J. Myers [125], J.W. Myrcha [142], B. Naik [48], R. Nair [83], B.K. Nandi [48], R. Nania [10,53], E. Nappi [52], M.U. Naru [15], A.F. Nassirpour [79], H. Natal da Luz [121], C. Nattrass [130], R. Nayak [48], T.K. Nayak [84,141], S. Nazarenko [107], R.A. Negrao De Oliveira [68], L. Nellen [69], S.V. Nesbo [36], G. Neskovic [39], B.S. Nielsen [87], S. Nikolaev [86], S. Nikulin [86], V. Nikulin [96], F. Noferini [10,53], P. Nomokonov [74], G. Nooren [63], J. Norman [77], P. Nowakowski [142], A. Nyanin [86], J. Nystrand [22], M. Ogino [80], A. Ohlson [102], J. Oleniacz [142], A.C. Oliveira Da Silva [121], M.H. Oliver [146], C. Oppedisano [58], R. Orava [43], A. Ortiz Velasquez [69], A. Oskarsson [79], J. Otwinowski [118], K. Oyama [80], Y. Pachmayer [102], V. Pacik [87], D. Pagano [140], G. Paić [69], P. Palni [6], J. Pan [143], A.K. Pandey [48], S. Panebianco [137], V. Papikyan [1], P. Pareek [49], J. Park [60], J.E. Parkkila [126], S. Parmar [98], A. Passfeld [144], S.P. Pathak [125], R.N. Patra [141], B. Paul [24,58], H. Pei [6], T. Peitzmann [63], X. Peng [6], L.G. Pereira [70], H. Pereira Da Costa [137], D. Peresunko [86], G.M. Perez [8], E. Perez Lezama [68], V. Peskov [68], Y. Pestov [4], V. Petráček [37], M. Petrovici [47], R.P. Pezzi [70], S. Piano [59], M. Pikna [14], P. Pillot [114], L.O.D.L. Pimentel [87], O. Pinazza [34,53], L. Pinsky [125], C. Pinto [28], S. Pisano [51], D.B. Piyarathna [125], M. Płoskoń [78], M. Planinic [97], F. Pliquett [68], J. Pluta [142], S. Pochybova [145], M.G. Poghosyan [94], B. Polichtchouk [89], N. Poljak [97], W. Poonsawat [115], A. Pop [47], H. Poppenborg [144], S. Porteboeuf-Houssais [134], V. Pozdniakov [74], S.K. Prasad [3], R. Preghenella [53], F. Prino [58], C.A. Pruneau [143], I. Pshenichnov [62], M. Puccio [26,34], V. Punin [107], K. Puranapanda [141], J. Putschke [143], R.E. Quishpe [125], S. Ragoni [109], S. Raha [3], S. Rajput [99], J. Rak [126], A. Rakotozafindrabe [137], L. Ramello [32], F. Rami [136], R. Raniwala [100], S. Raniwala [100], S.S. Räsänen [43], B.T. Rascanu [68], R. Rath [49], V. Ratza [42], I. Ravasenga [31], K.F. Read [94,130], K. Redlich [83,v], A. Rehman [22], P. Reichelt [68], F. Reidt [34], X. Ren [6], R. Renfordt [68], A. Reshetin [62], J.-P. Revol [10], K. Reygers [102], V. Riabov [96], T. Richert [79,87], M. Richter [21], P. Riedler [34], W. Riegler [34], F. Riggi [28], C. Ristea [67], S.P. Rode [49], M. Rodríguez Cahuantzi [44], K. Røed [21], R. Rogalev [89], E. Rogochaya [74], D. Rohr [34], D. Röhrich [22], P.S. Rokita [142], F. Ronchetti [51], E.D. Rosas [69], K. Roslon [142], P. Rosnet [134], A. Rossi [29], A. Rotondi [139], F. Roukoutakis [82], A. Roy [49], P. Roy [108], O.V. Rueda [79], R. Rui [25], B. Rumyantsev [74], A. Rustamov [85], E. Ryabinkin [86], Y. Ryabov [96], A. Rybicki [118], H. Rytkonen [126],

S. Sadhu [141], S. Sadovsky [89], K. Šafařík [34,37], S.K. Saha [141], B. Sahoo [48], P. Sahoo [48,49], R. Sahoo [49], S. Sahoo [65], P.K. Sahu [65], J. Saini [141], S. Sakai [133], S. Sambyal [99], V. Samsonov [91,96], A. Sandoval [71], A. Sarkar [72], D. Sarkar [143], N. Sarkar [141], P. Sarma [41], V.M. Sarti [103], M.H.P. Sas [63], E. Scapparone [53], B. Schaefer [94], J. Schambach [119], H.S. Scheid [68], C. Schiaua [47], R. Schicker [102], A. Schmah [102], C. Schmidt [105], H.R. Schmidt [101], M.O. Schmidt [102], M. Schmidt [101], N.V. Schmidt [68,94], A.R. Schmier [130], J. Schukraft [34,87], Y. Schutz [34,136], K. Schwarz [105], K. Schweda [105], G. Scioli [27], E. Scomparin [58], M. Šefčík [38], J.E. Seger [16], Y. Sekiguchi [132], D. Sekihata [45,132], I. Selyuzhenkov [91,105], S. Senyukov [136], D. Serebryakov [62], E. Serradilla [71], P. Sett [48], A. Sevcenco [67], A. Shabanov [62], A. Shabetai [114], R. Shahoyan [34], W. Shaikh [108], A. Shangaraev [89], A. Sharma [98], A. Sharma [99], H. Sharma [118], M. Sharma [99], N. Sharma [98], A.I. Sheikh [141], K. Shigaki [45], M. Shimomura [81], S. Shirinkin [90], Q. Shou [111], Y. Sibiriak [86], S. Siddhanta [54], T. Siemiarczuk [83], D. Silvermyr [79], C. Silvestre [77], G. Simatovic [88], G. Simonetti [34,103], R. Singh [84], R. Singh [99], V.K. Singh [141], V. Singhal [141], T. Sinha [108], B. Sitar [14], M. Sitta [32], T.B. Skaali [21], M. Slupecki [126], N. Smirnov [146], R.J.M. Snellings [63], T.W. Snellman [126], J. Sochan [116], C. Soncco [110], J. Song [60,125], A. Songmoolnak [115], F. Soramel [29], S. Sorensen [130], I. Sputowska [118], J. Stachel [102], I. Stan [67], P. Stankus [94], P.J. Steffanic [130], E. Stenlund [79], D. Stocco [114], M.M. Storetvedt [36], P. Strmen [14], A.A.P. Suaide [121], T. Sugitate [45], C. Suire [61], M. Suleymanov [15], M. Suljic [34], R. Sultanov [90], M. Šumbera [93], S. Sumowidagdo [50], K. Suzuki [113], S. Swain [65], A. Szabo [14], I. Szarka [14], U. Tabassam [15], G. Taillepied [134], J. Takahashi [122], G.J. Tambave [22], S. Tang [6,134], M. Tarhini [114], M.G. Tarzila [47], A. Tauro [34], G. Tejeda Muñoz [44], A. Telesca [34], C. Terrevoli [29,125], D. Thakur [49], S. Thakur [141], D. Thomas [119], F. Thoresen [87], R. Tieulent [135], A. Tikhonov [62], A.R. Timmins [125], A. Toia [68], N. Topilskaya [62], M. Toppi [51], F. Torales-Acosta [20], S.R. Torres [120], A. Trifiro [55], S. Tripathy [49], T. Tripathy [48], S. Trogolo [26,29], G. Trombetta [33], L. Tropp [38], V. Trubnikov [2], W.H. Trzaska [126], T.P. Trzcinski [142], B.A. Trzeciak [63], T. Tsuji [132], A. Tumkin [107], R. Turrisi [56], T.S. Tveter [21], K. Ullaland [22], E.N. Umaka [125], A. Uras [135], G.L. Usai [24], A. Utrobicic [97], M. Vala [38,116], N. Valle [139], S. Vallero [58], N. van der Kolk [63], L.V.R. van Doremalen [63], M. van Leeuwen [63], P. Vande Vyvre [34], D. Varga [145], Z. Varga [145], M. Varga-Kofarago [145], A. Vargas [44], M. Vargyas [126], R. Varma [48], M. Vasileiou [82], A. Vasiliev [86], O. Vázquez Doce [103,117], V. Vechernin [112], A.M. Veen [63], E. Vercellin [26], S. Vergara Limón [44], L. Vermunt [63], R. Vernet [7], R. Vértesi [145], M.G.D.L.C. Vicencio [9], L. Vickovic [35], J. Viinikainen [126], Z. Vilakazi [131], O. Villalobos Baillie [109], A. Villatoro Tello [44], G. Vino [52], A. Vinogradov [86], T. Virgili [30], V. Vislavicius [87], A. Vodopyanov [74], B. Volkel [34], M.A. Völkl [101], K. Voloshin [90], S.A. Voloshin [143], G. Volpe [33], B. von Haller [34], I. Vorobyev [103], D. Voscek [116], J. Vrláková [38], B. Wagner [22], Y. Watanabe [133], M. Weber [113], S.G. Weber [105,144], A. Wegrzynek [34], D.F. Weiser [102], S.C. Wenzel [34], J.P. Wessels [144], E. Widmann [113], J. Wiechula [68], J. Wikne [21], G. Wilk [83], J. Wilkinson [53], G.A. Willems [34], E. Willsher [109], B. Windelband [102], W.E. Witt [130], Y. Wu [128], R. Xu [6], S. Yalcin [76], K. Yamakawa [45], S. Yang [22], S. Yano [137], Z. Yin [6], H. Yokoyama [63,133], I.-K. Yoo [18], J.H. Yoon [60], S. Yuan [22], A. Yuncu [102], V. Yurchenko [2], V. Zaccolo [25,58], A. Zaman [15], C. Zampolli [34], H.J.C. Zanoli [63,121], N. Zardoshti [34], A. Zarochentsev [112], P. Závada [66], N. Zaviyalov [107], H. Zbroszczyk [142], M. Zhalov [96], X. Zhang [6], Z. Zhang [6], C. Zhao [21], V. Zherebchevskii [112], N. Zhigareva [90], D. Zhou [6], Y. Zhou [87], Z. Zhou [22], J. Zhu [6], Y. Zhu [6], A. Zichichi [10,27], M.B. Zimmermann [34], G. Zinovjev [2], N. Zurlo [140]

[1] *A.I. Alikhanyan National Science Laboratory (Yerevan Physics Institute) Foundation, Yerevan, Armenia*
[2] *Bogolyubov Institute for Theoretical Physics, National Academy of Sciences of Ukraine, Kiev, Ukraine*
[3] *Bose Institute, Department of Physics and Centre for Astroparticle Physics and Space Science (CAPSS), Kolkata, India*
[4] *Budker Institute for Nuclear Physics, Novosibirsk, Russia*
[5] *California Polytechnic State University, San Luis Obispo, CA, United States*
[6] *Central China Normal University, Wuhan, China*
[7] *Centre de Calcul de l'IN2P3, Villeurbanne, Lyon, France*
[8] *Centro de Aplicaciones Tecnológicas y Desarrollo Nuclear (CEADEN), Havana, Cuba*
[9] *Centro de Investigación y de Estudios Avanzados (CINVESTAV), Mexico City and Mérida, Mexico*
[10] *Centro Fermi – Museo Storico della Fisica e Centro Studi e Ricerche "Enrico Fermi', Rome, Italy*
[11] *Chicago State University, Chicago, IL, United States*
[12] *China Institute of Atomic Energy, Beijing, China*
[13] *Chonbuk National University, Jeonju, Republic of Korea*
[14] *Comenius University Bratislava, Faculty of Mathematics, Physics and Informatics, Bratislava, Slovakia*
[15] *COMSATS University Islamabad, Islamabad, Pakistan*
[16] *Creighton University, Omaha, NE, United States*
[17] *Department of Physics, Aligarh Muslim University, Aligarh, India*
[18] *Department of Physics, Pusan National University, Pusan, Republic of Korea*
[19] *Department of Physics, Sejong University, Seoul, Republic of Korea*
[20] *Department of Physics, University of California, Berkeley, CA, United States*
[21] *Department of Physics, University of Oslo, Oslo, Norway*

[22] Department of Physics and Technology, University of Bergen, Bergen, Norway
[23] Dipartimento di Fisica dell'Università 'La Sapienza' and Sezione INFN, Rome, Italy
[24] Dipartimento di Fisica dell'Università and Sezione INFN, Cagliari, Italy
[25] Dipartimento di Fisica dell'Università and Sezione INFN, Trieste, Italy
[26] Dipartimento di Fisica dell'Università and Sezione INFN, Turin, Italy
[27] Dipartimento di Fisica e Astronomia dell'Università and Sezione INFN, Bologna, Italy
[28] Dipartimento di Fisica e Astronomia dell'Università and Sezione INFN, Catania, Italy
[29] Dipartimento di Fisica e Astronomia dell'Università and Sezione INFN, Padova, Italy
[30] Dipartimento di Fisica 'E.R. Caianiello' dell'Università and Gruppo Collegato INFN, Salerno, Italy
[31] Dipartimento DISAT del Politecnico and Sezione INFN, Turin, Italy
[32] Dipartimento di Scienze e Innovazione Tecnologica dell'Università del Piemonte Orientale and INFN Sezione di Torino, Alessandria, Italy
[33] Dipartimento Interateneo di Fisica 'M. Merlin' and Sezione INFN, Bari, Italy
[34] European Organization for Nuclear Research (CERN), Geneva, Switzerland
[35] Faculty of Electrical Engineering, Mechanical Engineering and Naval Architecture, University of Split, Split, Croatia
[36] Faculty of Engineering and Science, Western Norway University of Applied Sciences, Bergen, Norway
[37] Faculty of Nuclear Sciences and Physical Engineering, Czech Technical University in Prague, Prague, Czech Republic
[38] Faculty of Science, P.J. Šafárik University, Košice, Slovakia
[39] Frankfurt Institute for Advanced Studies, Johann Wolfgang Goethe-Universität Frankfurt, Frankfurt, Germany
[40] Gangneung-Wonju National University, Gangneung, Republic of Korea
[41] Gauhati University, Department of Physics, Guwahati, India
[42] Helmholtz-Institut für Strahlen- und Kernphysik, Rheinische Friedrich-Wilhelms-Universität Bonn, Bonn, Germany
[43] Helsinki Institute of Physics (HIP), Helsinki, Finland
[44] High Energy Physics Group, Universidad Autónoma de Puebla, Puebla, Mexico
[45] Hiroshima University, Hiroshima, Japan
[46] Hochschule Worms, Zentrum für Technologietransfer und Telekommunikation (ZTT), Worms, Germany
[47] Horia Hulubei National Institute of Physics and Nuclear Engineering, Bucharest, Romania
[48] Indian Institute of Technology Bombay (IIT), Mumbai, India
[49] Indian Institute of Technology Indore, Indore, India
[50] Indonesian Institute of Sciences, Jakarta, Indonesia
[51] INFN, Laboratori Nazionali di Frascati, Frascati, Italy
[52] INFN, Sezione di Bari, Bari, Italy
[53] INFN, Sezione di Bologna, Bologna, Italy
[54] INFN, Sezione di Cagliari, Cagliari, Italy
[55] INFN, Sezione di Catania, Catania, Italy
[56] INFN, Sezione di Padova, Padova, Italy
[57] INFN, Sezione di Roma, Rome, Italy
[58] INFN, Sezione di Torino, Turin, Italy
[59] INFN, Sezione di Trieste, Trieste, Italy
[60] Inha University, Incheon, Republic of Korea
[61] Institut de Physique Nucléaire d'Orsay (IPNO), Institut National de Physique Nucléaire et de Physique des Particules (IN2P3/CNRS), Université de Paris-Sud, Université Paris-Saclay, Orsay, France
[62] Institute for Nuclear Research, Academy of Sciences, Moscow, Russia
[63] Institute for Subatomic Physics, Utrecht University/Nikhef, Utrecht, Netherlands
[64] Institute of Experimental Physics, Slovak Academy of Sciences, Košice, Slovakia
[65] Institute of Physics, Homi Bhabha National Institute, Bhubaneswar, India
[66] Institute of Physics of the Czech Academy of Sciences, Prague, Czech Republic
[67] Institute of Space Science (ISS), Bucharest, Romania
[68] Institut für Kernphysik, Johann Wolfgang Goethe-Universität Frankfurt, Frankfurt, Germany
[69] Instituto de Ciencias Nucleares, Universidad Nacional Autónoma de México, Mexico City, Mexico
[70] Instituto de Física, Universidade Federal do Rio Grande do Sul (UFRGS), Porto Alegre, Brazil
[71] Instituto de Física, Universidad Nacional Autónoma de México, Mexico City, Mexico
[72] iThemba LABS, National Research Foundation, Somerset West, South Africa
[73] Johann-Wolfgang-Goethe Universität Frankfurt Institut für Informatik, Fachbereich Informatik und Mathematik, Frankfurt, Germany
[74] Joint Institute for Nuclear Research (JINR), Dubna, Russia
[75] Korea Institute of Science and Technology Information, Daejeon, Republic of Korea
[76] KTO Karatay University, Konya, Turkey
[77] Laboratoire de Physique Subatomique et de Cosmologie, Université Grenoble-Alpes, CNRS-IN2P3, Grenoble, France
[78] Lawrence Berkeley National Laboratory, Berkeley, CA, United States
[79] Lund University Department of Physics, Division of Particle Physics, Lund, Sweden
[80] Nagasaki Institute of Applied Science, Nagasaki, Japan
[81] Nara Women's University (NWU), Nara, Japan
[82] National and Kapodistrian University of Athens, School of Science, Department of Physics, Athens, Greece
[83] National Centre for Nuclear Research, Warsaw, Poland
[84] National Institute of Science Education and Research, Homi Bhabha National Institute, Jatni, India
[85] National Nuclear Research Center, Baku, Azerbaijan
[86] National Research Centre Kurchatov Institute, Moscow, Russia
[87] Niels Bohr Institute, University of Copenhagen, Copenhagen, Denmark
[88] Nikhef, National institute for subatomic physics, Amsterdam, Netherlands
[89] NRC Kurchatov Institute IHEP, Protvino, Russia
[90] NRC "Kurchatov Institute" – ITEP, Moscow, Russia
[91] NRNU Moscow Engineering Physics Institute, Moscow, Russia
[92] Nuclear Physics Group, STFC Daresbury Laboratory, Daresbury, United Kingdom
[93] Nuclear Physics Institute of the Czech Academy of Sciences, Řež u Prahy, Czech Republic
[94] Oak Ridge National Laboratory, Oak Ridge, TN, United States
[95] Ohio State University, Columbus, OH, United States
[96] Petersburg Nuclear Physics Institute, Gatchina, Russia
[97] Physics department, Faculty of science, University of Zagreb, Zagreb, Croatia
[98] Physics Department, Panjab University, Chandigarh, India
[99] Physics Department, University of Jammu, Jammu, India
[100] Physics Department, University of Rajasthan, Jaipur, India

[101] Physikalisches Institut, Eberhard-Karls-Universität Tübingen, Tübingen, Germany
[102] Physikalisches Institut, Ruprecht-Karls-Universität Heidelberg, Heidelberg, Germany
[103] Physik Department, Technische Universität München, Munich, Germany
[104] Politecnico di Bari, Bari, Italy
[105] Research Division and ExtreMe Matter Institute EMMI, GSI Helmholtzzentrum für Schwerionenforschung GmbH, Darmstadt, Germany
[106] Rudjer Bošković Institute, Zagreb, Croatia
[107] Russian Federal Nuclear Center (VNIIEF), Sarov, Russia
[108] Saha Institute of Nuclear Physics, Homi Bhabha National Institute, Kolkata, India
[109] School of Physics and Astronomy, University of Birmingham, Birmingham, United Kingdom
[110] Sección Física, Departamento de Ciencias, Pontificia Universidad Católica del Perú, Lima, Peru
[111] Shanghai Institute of Applied Physics, Shanghai, China
[112] St. Petersburg State University, St. Petersburg, Russia
[113] Stefan Meyer Institut für Subatomare Physik (SMI), Vienna, Austria
[114] SUBATECH, IMT Atlantique, Université de Nantes, CNRS-IN2P3, Nantes, France
[115] Suranaree University of Technology, Nakhon Ratchasima, Thailand
[116] Technical University of Košice, Košice, Slovakia
[117] Technische Universität München, Excellence Cluster 'Universe', Munich, Germany
[118] The Henryk Niewodniczanski Institute of Nuclear Physics, Polish Academy of Sciences, Cracow, Poland
[119] The University of Texas at Austin, Austin, TX, United States
[120] Universidad Autónoma de Sinaloa, Culiacán, Mexico
[121] Universidade de São Paulo (USP), São Paulo, Brazil
[122] Universidade Estadual de Campinas (UNICAMP), Campinas, Brazil
[123] Universidade Federal do ABC, Santo Andre, Brazil
[124] University of Cape Town, Cape Town, South Africa
[125] University of Houston, Houston, TX, United States
[126] University of Jyväskylä, Jyväskylä, Finland
[127] University of Liverpool, Liverpool, United Kingdom
[128] University of Science and Technology of China, Hefei, China
[129] University of South-Eastern Norway, Tonsberg, Norway
[130] University of Tennessee, Knoxville, TN, United States
[131] University of the Witwatersrand, Johannesburg, South Africa
[132] University of Tokyo, Tokyo, Japan
[133] University of Tsukuba, Tsukuba, Japan
[134] Université Clermont Auvergne, CNRS/IN2P3, LPC, Clermont-Ferrand, France
[135] Université de Lyon, Université Lyon 1, CNRS/IN2P3, IPN-Lyon, Villeurbanne, Lyon, France
[136] Université de Strasbourg, CNRS, IPHC UMR 7178, F-67000 Strasbourg, France
[137] Université Paris-Saclay Centre d'Etudes de Saclay (CEA), IRFU, Département de Physique Nucléaire (DPhN), Saclay, France
[138] Università degli Studi di Foggia, Foggia, Italy
[139] Università degli Studi di Pavia, Pavia, Italy
[140] Università di Brescia, Brescia, Italy
[141] Variable Energy Cyclotron Centre, Homi Bhabha National Institute, Kolkata, India
[142] Warsaw University of Technology, Warsaw, Poland
[143] Wayne State University, Detroit, MI, United States
[144] Westfälische Wilhelms-Universität Münster, Institut für Kernphysik, Münster, Germany
[145] Wigner Research Centre for Physics, Hungarian Academy of Sciences, Budapest, Hungary
[146] Yale University, New Haven, CT, United States
[147] Yonsei University, Seoul, Republic of Korea

[i] Deceased.
[ii] Dipartimento DET del Politecnico di Torino, Turin, Italy.
[iii] M.V. Lomonosov Moscow State University, D.V. Skobeltsyn Institute of Nuclear, Physics, Moscow, Russia.
[iv] Department of Applied Physics, Aligarh Muslim University, Aligarh, India.
[v] Institute of Theoretical Physics, University of Wroclaw, Poland.